C/ORNL/94-0301

ornl

OAK RIDGE NATIONAL LABORATORY

LOCKHEED MARTIN

CRADA Final Report
for
CRADA Number ORNL 94-0301

IMPROVED MINERAL INSULATION CABLES FOR HIGH RADIATION ENVIRONMENTS

STTR TOPIC NO. 9.0 B
CONTRACT No. DE-FGO5-94ER86002

DR. LANCE SNEAD
OAK RIDGE NATIONAL LABORATORY

AND

R. W. MCCULLOCH
J. P. STAMP
DELTA M CORPORATION

DECEMBER 21, 1995

Prepared by the
Oak Ridge National Laboratory
Oak Ridge, Tennessee 37831-6087
Managed by
Lockheed Martin Energy Research Corp.
For the
U.S. Department of Energy
under contract DE-AC05-96OR22464

Report Prepared in Fulfillment of the Requirements of the Small Business Technology Transfer Program (STTR) by the U.S. Department of Energy

Protected CRADA Information

This product contains Protected CRADA Information which was produced on December 21, 1995 under CRADA No. ORNL/94-0301 and is not to be further disclosed for a period of five (5) years from the date it was produced except as expressly provided for in the CRADA.

MANAGED AND OPERATED BY
LOCKHEED MARTIN ENERGY RESEARCH CORPORATION
FOR THE UNITED STATES
DEPARTMENT OF ENERGY

ORNL-27 (3-96)

C/ORNL/94-0301

CRADA Final Report
for
CRADA Number ORNL 94-0301

IMPROVED MINERAL INSULATION CABLES FOR HIGH RADIATION ENVIRONMENTS

STTR TOPIC NO. 9.0 B
CONTRACT No . DE-FGO5-94ER86002

DR. LANCE SNEAD
OAK RIDGE NATIONAL LABORATORY

AND

R. W. MCCULLOCH
J. P. STAMP
DELTA M CORPORATION

DECEMBER 21, 1995

Prepared by the
Oak Ridge National Laboratory
Oak Ridge, Tennessee 37831-6087
Managed by
Lockheed Martin Energy Research Corp.
For the
U.S. Department of Energy
under contract DE-AC05-96OR22464

Report Prepared in Fulfillment of the Requirements of the Small Business Technology Transfer Program (STTR) by the U.S. Department of Energy

Protected CRADA Information

PROJECT SUMMARY

The use of insulating cables for applications in high radiation fields has become problematic due to the breakdown in electrical properties of the insulating materials used. Generally, for applications with modest ionizing or displacive radiation fields the use of mineral insulated cables is required. In many nuclear applications, however, a sizeable immediate degradation occurs which can render components such as diagnostic probes useless. As example, magnetic diagnostics are of critical importance for the operation of tokamaks such as the International Thermonuclear Experimental Reactor (ITER) machine. Due to the enhanced gamma and neutron flux expected in the ITER machine, analysis has shown that sensor types proposed in the Conceptual Design Phase of ITER and by the ITER Joint Central Team are basically inadequate.

The purpose of this work was to develop improved mineral insulated cables with decreased radiation induced electrical conductivities (RIC), specifically to develop a cable with conductivity $<1 \times 10^{-7}$ S/m at a dose rate of 10^4 Gy/s.

The research included: (1) selection of starting materials with low intrinsic RIC and (2) optimization of the processing parameters to develop viable low leakage cables for nuclear environments. Insulation materials selected included alumina, mullite, cordierite, and diamond. Candidate cables were irradiated at the Gaertner linear accelerator at Rensselaer Polytechnic Institute. Dose rates of 0.7, 7.0, and 42 Gy/s were obtained.

This Phase I effort demonstrated that mineral insulated coaxial cables, would meet the primary technical objective of $<10^{-7}$ S/m at tokamak-relevant radiation cases with the appropriate selection of insulating material. Two alumina insulated cables had extrapolated conductivities of approximately 10^{-9} S/m at 10^4 Gy/s which is a dose rate typical of fission power systems, that expected for fusion machines such as ITER, and approximately one order of magnitude higher that many research accelerators. Additionally, a fundamental knowledge of the mechanisms responsible for conduction in these cables was obtained and a technology base for fabrication of these cables was developed.

The primary potential application of the improved mineral insulated cable is for magnetic diagnostics for fusion reactor programs. Other applications include accelerators, commercial nuclear reactors, and Naval nuclear reactors.

ABSTRACT

The use of insulating cables for applications in high radiation fields has become problematic due to the breakdown in electrical properties of the insulating materials used. Generally, for applications with modest ionizing or displacive radiation fields the use of mineral insulated cables is required. In many nuclear applications, however, a sizeable immediate degradation occurs which can render components such as diagnostic probes useless. As example, magnetic diagnostics are of critical importance for the operation tokamaks such as the International Thermonuclear Experimental Reactor (ITER) machine. Due to the enhanced gamma and neutron flux expected in the ITER machine, analysis has shown that sensor types proposed in the Conceptual Design Phase of ITER and by the ITER Joint Central Team are basically inadequate.

The Phase I effort demonstrated that mineral insulated coaxial cables, one half the typical diameter of previous cables, would meet the primary technical objective of $<10^{-7}$ S/m at tokamak-relevant radiation cases. Two alumina insulated cables had extrapolated conductivities of approximately 10^{9} S/m at 10^{4} Gy/s which is a dose rate typical of fission power systems, that expected for fusion machines such as ITER, and approximately one order of magnitude higher than many research accelerators. Additionally, a fundamental knowledge of the mechanisms responsible for conduction in these cables was obtained and a technology base for fabrication of these cables was developed. These two achievements will provide a basis for informed optimization of a low radiation induced conductivity (RIC) product in future research.

TABLE OF CONTENTS

LIST OF TABLES

LIST OF FIGURES

1.0 INTRODUCTION

This report presents the results of a STTR Phase I performed jointly by DELTA M Corporation and the Oak Ridge National Laboratory (ORNL) for the U. S. Department of Energy (DOE) on improved mineral insulated cables for high radiation environments.

The use of insulating cables for applications in high radiation fields has become problematic due to the breakdown in electrical properties of the insulating materials used. Generally, for any application with modest ionizing or displacive radiation fields the use of mineral insulated cables is required. However, mineral insulated cables have a sizable immediate degradation in resistively which can compromise the low level current measurements required in many applications. As example, magnetic diagnostics are of critical importance for the operation of tokamaks such as the DOE-sponsored International Thermonuclear Experimental Reactor (ITER) machine. The ITER baseline magnetic diagnostic design uses mineral insulated (MI) cable as the main component in the construction of the magnetic loop probes. Of principle concern in this design is the leakage current induced in the cables during the high-radiation pulses. Currently available MI cable has been shown (Ref. 1) to be inadequate. A reduction in conductivity of at least one order of magnitude is required, with a preference (Ref. 2) for an overall conductivity of $< 10^{-7}$ S/m at relevant first wall dose levels. As this application is an ideal candidate to prove the benefits at improved mineral isolated cables, it has been selected as the test-base for the Phase II development.

While the mineral insulation used in cables and sensors starts with exceedingly low conductivities ($<<10^{-10}$ S/m), the effect of ionizing radiation is to enhance this conductivity by as much as several orders of magnitude. As example, bulk magnesium oxide, which is the most commonly used powder in mineral insulated cables, has been shown (Ref. 3) to increase in conductivity from an unirradiated value of $<<10^{-13}$ S/m to about 10^{-6} S/m at gamma fluxes of 10^4 Gy/s. This phenomena has been well studied in bulk oxide ceramics and is called radiation induced conductivity (RIC). It is caused by the excitation of electrons into the conduction band of the insulator by ionizing radiation (typically gamma). This effect is essentially temperature independent but varies widely not only for different ceramic types but also for varying dopant levels and crystalline forms of "like" ceramics.

In the Phase I effort, DELTA M Corporation, in conjunction with the Oak Ridge National Laboratory, fabricated and tested a series of mineral insulated cables with a range of properties suitable to better define the RIC phenomena and to achieve a one to two order of magnitude decrease in the conductivity at first wall relevant gamma fluxes of 10^4 Gy/s. The results of Phase I, are summarized as follows.

1. A cable geometry of 1.5 mm outer diameter with a 0.25-mm diameter inner conductor was selected. This miniature cable is half the diameter of most previous cables and is identical to cables recently used by General Atomics which were helically wound to form a diagnostic probe for testing in a high radiation environment. A smaller diameter cable is lighter, more flexible, and better fits the limited space requirements.

2. Techniques were developed to powder fill the insulation materials instead of using crushable preforms. Powder filling eliminates the powder extrusion step which potentially reduces impurity levels and provides better defined powder grain size distribution of the final product.

3. Techniques were developed to control the initial compaction density of the insulation and to monitor and control the rate of compaction during processing. These were necessary to optimize fabrication using a wide range of powder types and characteristics and will provide an important technology base for future cable fabrication.

4. The feasibility of doping polycrystalline ceramics was demonstrated by adding 0.01, 0.1 and 1% weight percent chromia to high purity alumina. However, the effect of doping on the RIC could not be ascertained due to an increase in the base-line (no radiation-induced) conductivity.

5. Following several failed attempts to fabricate small diameter S_iO_2, cables, further development of a glass MI cable was deferred. However specimens containing $3Al_2O_3{\cdot}2S_iO_2$(Mullite) and $2Mg0{\cdot}Al_2O_3{\cdot}5S_iO_2$ (Cordierite) were successfully fabricated and tested. A major effort in future work will be to develop appropriate fabrication techniques to manufacture high quality S_iO_2 insulated cables.

6. The primary technical objective of demonstrating a mineral insulated coaxial cable with $<10^{-7}$ S/m at tokamak-relevant radiation doses was successfully met. Providing that the diagnostic in question can be kept below 450°C, two candidate alumina insulated cables are expected to have conductivities of approximately 10^{-9} S/m at 10^4 Gy/s.

7. A fundamental knowledge of the mechanisms responsible for conduction in these mineral insulated cables was obtained and will lead to informed optimization in future related research.

2.0 BACKGROUND

There is a growing need for diagnostic sensors for general measurement and control instrumentation in high radiation environments such as nuclear power systems, accelerator based machines and nuclear waste tanks. One common problem in such environments is the permanent degradation in organically insulated cabling and the transient degradation in the electrical properties of mineral insulated cables.

Helically wound mineral insulated cables are currently in use in fusion reactors such a D-III D as magnetic diagnostics. A typical semi-rigid coaxial probe is shown in Figure 1. When used in a gamma irradiation field the leakage current across the insulation of the coaxial cable is significantly increased due to the radiation induced conductivity (RIC) in the insulating barrier. This phenomenon is transient, i.e. only present during the irradiation, and is caused by ionization of electrons into the previously unpopulated conduction band of the ceramic. RIC has been demonstrated in many insulating ceramics and glasses and is given in Figure 2 over a range of radiation dose rates.

From Figure 2 it is seen that the RIC effect is linear with dose rate and shows no sign of saturation at dose rates greater than that expected for fusion machines. It can be seen from this data set that for alumina, magnesium oxide and spinel, the conductivity has increased several orders of magnitude in the dose rate range of interest for fusion reactors. As a specific example, alumina is seen to increase in conductivity from $<10^{-12}$ S/m in the unirradiated state, to about 10^{-6} S/m at a dose rate of 10^4 Gy/s.

The mechanism behind the increase in conductivity of these insulating materials has to do with the radiation induced excitation of electrons into the previously unpopulated conduction band. This mechanism therefore causes a transient change in electrical conductivity and the material is restored to its "base"' conductivity

once the radiation source is eliminated. For dose rates of interest to fusion, it has been assumed that these radiation induced conduction electrons would far outnumber any thermally induced conduction electrons.

As will be seen later, thermal effects can be quite important and will be a prime driver in the selection of insulators. However, the RIC component of conductivity itself is seen to be temperature independent.

A wide scatter in RIC is seen not only from material to material, but within like materials. Figure 2 shows significant scatter in the oxide. Not shown in Figure 2 is a limited data set on RIC in glasses which shows about an order of magnitude lower conductivity. The effect of scatter in like materials has been shown for single crystal and polycrystalline alumina as well as for doped alumina. In the case of doping, it was shown that 0.03 weight percent Cr_2O_3, caused a two order of magnitude decrease in the RIC for , single crystal alumina (Ref. 4 and 5) at room temperature.

In the past few years there have been several papers on a potentially more serious problem relating to the use of insulating ceramics in fusion systems (Ref. 6-13). Three separate research groups (Ref 7-13) have published studies in which electrical conductivity was measured in the presence of ionizing and displacive radiation fields while an electrical field was applied. The results of these studies indicated that in addition to the well-established increase in conductivity (RIC) , a permanent increase in conductivity occurs which greatly exceeds the RIC value after some threshold fluence is reached. The point at which the permanent conductivity began to increase above the RIC level varied from approximately 2×10^{-5} dpa for electron irradiation (Ref. 12), 1×10^{-3} dpa for proton irradiation (Ref. 8) and 3×10^{-2} dpa for fission neutron irradiation (Ref. 11) near 500°C. This effect has been classified as radiation induced electrical degradation (RIED) and has to this point not exhibited an upper limit in conductivity. Figure 3 shows a compilation of data on the RIED effect and shows the dramatic increase in conductivity after the threshold dose has been reached. While there has not been a systematic study of the variables underlying this effect, it is known that an applied electric field is necessary during irradiation, and there is evidence suggesting that RIED does not occur below 200°C or above 650°C (Refs. 9, 10, 14). It is also important to note that there has been significant recent work which suggests that by appropriate selection of the type of insulator chosen (Wesgo AL-995) RIED does not occur at fusion temperatures and doses (Ref.14) relevant to the ITER machine.

3.0 SCOPE AND TECHNICAL OBJECTIVES

This Phase I study was undertaken in response to a DOE need for improved mineral insulated cable (MIC) in high radiation (gamma fluxes of 10^4 Gy/s) environments.

3.1 SCOPE

The scope of the Phase I effort was to assume a single coaxial geometry similar to, but smaller than, the existing ITER diagnostic coil designs, examine a variety of ceramic insulators that indicate promise for improved MIC properties, and build on the present fabrication base established at DELTA M to obtain at least a two orders of magnitude improvement in insulation properties. Cables were to be evaluated to determine RIC versus radiation dose by ORNL.

3.2 PHASE I TECHNICAL OBJECTIVES

The specific purpose of the Phase I effort was to fabricate a number of high quality coaxial cables using a variety of ceramic and/or glass powders, form the cables into the ITER diagnostic helically coiled configuration, and demonstrate a radiation-induced conductivity of $<10^{-7}$ S/m at a fusion relevant dose rate of 10^4 Gy/s. A further reduction of one to two orders of magnitude below this goal was considered highly desirable. In addition to demonstrating a cable with the requirements listed above, an emphasis of this research was an understanding of the basic mechanisms behind the conduction in mineral insulated cables to better guide future research. These objectives were pursued through the several tasks described in Section 4.0 following.

4.0 DESCRIPTION OF TECHNICAL WORK PERFORMED AND COMMERCIALIZATION ROUTE

This section presents the results obtained in this study on a task by task basis. The task is stated and specific accomplishments are presented and discussed. In cases where information is multi-task oriented, the results are described under one task with reference to others.

4.1 TASK 1: MATERIALS SELECTION AND EXPERIMENTAL RATIONALE

Task statement. Review and update selection criteria of insulation materials, determine the feasibility of doping materials, and evaluate any other information pertinent to improved ITER diagnostics. Coordinate with diagnostic experts to determine adequacy of the research program.

Results. Before final selection of materials and processes, a thorough study was conducted to determine candidate materials and into the feasibility of doping polycrystalline ceramics. Concurrently, process studies were initiated to examine the best methods to maintain high purity and process control. During this period the material matrix and experimental plan was discussed with members of the fusion community to ensure an adequate Phase I program.

Results of the materials study provided relevant new information including:

1. It quickly became apparent that, due to the uncertainty in the application temperature for many diagnostic systems, temperature must be added as a variable to the research program.

2. In order to accommodate including temperature as a variable the sample matrix was reduced to the four most promising
material families: alumina (including cordierite and mullite), magnesium oxide, glass and diamond. Spinel was dropped from Phase I and is proposed for Phase II.

3. As it has been shown by previous researchers that RIC could be significantly reduced in bulk alumina by chromia-doping of single crystal alumina, the possible production of chromia doped gamma alumina was explored. It was determined to be feasible and was pursued.

4. It was decided that only high purity materials would be pursued in Phase I to eliminate potential variables.

Results of process studies provided several important inputs including:

1. For best results powders should be stored above 100°C.

2. After the insulation material is loaded into the sheath the assembly should be heated overnight in vacuum at a temperature of at least 450°C before further processing.

3. Powder filling will result in lower impurity levels and better knowledge of the particle size distribution than using extruded preforms.

4. Reduction to final diameter by a combination of swaging and annealing provided a better means of process control over the anticipated wide range of powder types.

5. Measurement of the elongation and diameter change at each reduction pass, and calculation of the insulation compaction density as a function of diameter, is a useful way to evaluate the potential of reduction processes on new powder types.

This information was employed in the final selection of materials and processes as delineated in Task 2.

4.2 TASK 2: SELECTION OF INSULATING MATERIALS AND PROCESS PARAMETERS

Task Statement. Select specific candidate insulation materials including type, purity, and particle size distribution. Determine best processing methods and evaluation techniques to maintain high purity levels, accommodate a wide range of material, and control final densities. If feasible, determine candidate dopants, dopant levels and dopant methods.

Results. The information obtained from Task I was used to determine a new matrix of candidate materials. Table I shows the candidate materials selected.

Table 1. Materials Selected for Evaluation—Insulation Materials

Al_2O_3	MgO	Cr_2O_3 Doped Alumina	Al_2O_3-MgO-SiO_2+ Diamond	SiO_2
Ultrafine PSD*	Medium PSD	1% C_R	Mullite	Quartz
Fine PSD	Course PSD	0.1% C_R	Cordierite	Pb-B-SiO_2
Course PSD		0.1% C_R	Diamond	

PSD* = particle size distribution

All high purity ceramics were supplied by Baikowski International in powder form. The standard MgO and Al_2O_3 were supplied by Ozark Technical Ceramics and the type 1B synthetic diamond powder was supplied by Harris Diamond. It was believed that by utilizing primarily Baikowski high purity powders along with powder loading techniques, impurity levels could be minimized.

A powder filling device was designed, fabricated and tested. It applied standard powder filling techniques but had provisions for tamping loaded powder to control the filled density.

A series of prototypes was assembled and processed in an attempt to determine the range of processing parameters applicable to the materials selected. It was determined that a combination of swaging and drawing passes was required for optimal reduction from the starting diameter of 8.8 mm to the final diameter of 1.5 mm. After each pass the assembly was annealed at conditions selected to obtain full recrystallization of the copper conductor and stainless steel sheath.

A standard process was finally determined that applied to all powdered materials of Table 1 except diamond and the silicas. This process consisted of three initial swaging passes, each with an anneal, followed by drawing passes until the final diameter was reached. The process for the diamond insulated material required an initial draw pass, followed by three swaging passes, then by subsequent draw passes. The final diameter of the diamond sample was 1.9 mm instead of 1.5 mm. Further processing would have resulted in failure of the sample.

The silica samples were initially processed in much the same way as the other samples but this resulted in poor quality samples. Quality of the samples was found to be sensitive to the amount of reduction per pass, reduction method (swaging or drawing) , and annealing parameters. Failure was normally due to excessive abrasion of the center copper conductor by the silica.

Because of continued problems with obtaining samples with SiO_2 insulation, these samples were eliminated from the test matrix of materials to be radiation tested on Phase I. Development is continuing and samples will be made available for radiation testing as part of the Phase II effort.

Process control was conducted through: (1) examination of radiographs taken at selected diameters during the reduction; (2) measurement of sheath outer diameter (OD), inner diameter (ID) and conductor diameter at selected processing stages; and (3) calculation of the insulation density-vs-diameter using the information from (2).

Figures 4a and b show photographs of longitudinal radiographs of (a) a successfully fabricated coaxial cable, and (b) and unsuccessfully fabricated coaxial cable. In both cases the top photograph was obtained immediately after loading and the bottom photograph was obtained during the process. The sheath walls and center copper conductor show up on the radiograph as bright areas; the insulation is the darker regions. The unsuccessful cable in Figure 4b (SiO_2) failed by abrasion of the center conductor and by cracking of the sheath. By comparison, the center conductor and sheath are much more uniform in the processed sample of 4a.

At selected diameters a short sample was cut from each coaxial assembly, the sample was sectioned, and the sheath ID and conductor diameter were measured. These values, along with the sheath OD, were used to calculate the insulation material density as a function of reduction diameter. Data from a range of samples led to two general conclusions about the processes for Al_2O_3, MgO, doped Al_2O_3, and the Al_2O_3/MgO/SiO_2 combinations:

1. The final density was a parameter that could not be controlled. Rather it appeared to be primarily a function of the particle size distribution.

2. If the transition range in density was too sharp it usually resulted in sample failure.

Although the starting density could be controlled within a range, if it was too high the transition to final density was sharp and the insulation material damaged the sheath wall and conductor. Thus the optimized process included a relatively low starting density with controlled swaging and drawing steps to result in a smooth transition to a higher final density. Figure 5 plots the calculated change in density with diameter for two insulation materials. In both the transition in density is gradual, occurring over a diameter range of nine to four mm.

After the cable assemblies were completed they were cut to length, sealed, and their insulation resistance was measured. For each material, three samples were obtained for destructive testing. Dielectric breakdown tests were performed on the first sample. Micrographs were obtained for dimensional measurements on the second and the third was evaluated per ASTM D2771-69, Method B for determination of insulation material density. The full length cables were then wound on a mandrel into the diagnostic configuration for irradiation testing and the insulation resistance of each cable was remeasured. Table 2 provides a compilation of electrical and dimensional data on the cables and Table 3 shows insulation material properties such as final density, bulk density, purity, surface area, and particle size distribution.

An important artifact of the drawing and swaging process typical of all mineral insulated cables is given in the photomicrographs of Figures 6a and 6b. Both of these samples are magnesium oxide with an outer diameter of 1.52 mm and an outer 316 stainless steel sheath thickness of approximately 0.2 mm. It is seen in Figure 6a that there is non-uniformity along the circumference of the copper conductor, and to a lesser extent on the inner diameter of the stainless steel sheath. These irregularities are actual striations which run longitudinally along the cable, and can be reduced or enhanced by varying both the drawing and swaging process, though the swaging process is more damaging. Figure 6b shows a more exaggerated non-uniformity in the copper center conductor and it is expected that further swaging of this conductor would have caused a cable failure. It should be noted as well that the insulation size and type has a dramatic influence on the amount of damage to the center conductor, as demonstrated by the difficulty in fabricating both the glass and diamond insulated cables.

Photomicrographs such as those shown in Figures 6a and 6b were used in the evaluation of the drawing/swaging process to determine swaging steps as well as used to give final dimensions of sheath ID and conductor OD. The dimensional data as well as the physical properties of the cables are given in Tables 2 and 3. It should be noted that the outer diameter of the sheath was taken to be a mean in the case of irregular conductors. Due to the relatively large insulation thickness the non-uniformity in the center conductor should have a negligible effect on the electric field of the cable, though this would not be the case for very jagged center conductors and much thinner insulating thickness.

4.3 TASK 3: IRRADIATION TESTING

Task Statement. Perform measurements on helically wound specimens of candidate cables at dose rates adequate to simulate fusion conditions. Measure leakage current and bulk conductivity across the insulating material under an applied DC field. Compare irradiated material data with unirradiated measurements and determine that no permanent degradation has taken place.

TABLE 2 ELECTRICAL AND DIMENSIONAL DATA OF SELECTED COAXIAL CABLES

DESIGNATION	INITIAL RT IR @ 10 VDC	COILED RT IR @ 10 VDC	SHEATH OD, mm	SHEATH ID, mm	CONDUCTOR OD, mm	DIELECTRIC BREAKDOWN KV/mm
	G OHMS	G OHMS				
411H, CR125, HPAl_2O_3[b]	1000	1000	1.52	1.19	0.16	4.85[a]
666L, CR1, HPAl_2O_3	120	125	1.52	1.23	0.24	5.05[a]
4059, 1%C_r, CR125	140	140	1.52	1.07	0.17	5.55[a]
4060, .1%C_r, CR125	120	120	1.52	1.05	0.15	4.0
4061, .01%C_r, CR125	115	120	1.52	1.16	0.17	5.05[a]
STANDARD Al_2O_3	170	165	1.61	1.24	0.26	4.85[a]
STANDARD MgO	144	140	1.52	1.13	0.22	5.49[a]
907, HP MgO	140	140	1.52	1.12	0.31	6.17[a]
6655 HP CORDIERITE	770	800	1.52	1.32	0.14	4.23[a]
6986 HP MULLITE	135	130	1.52	1.36	0.14	3.77
HP DIAMOND	70	65	1.88	1.62	0.16	N/A

[a] NO FAILURE AT V_{MAX} = 2.5KV

[b] HP = HIGH PURITY

TABLE 3 PROPERTIES OF SELECTED INSULATION MATERIALS

DESIGNATION	BULK DENSITY g/cm³	FINAL DENSITY g/cm³	FINAL % ID	PURITY (%)	SURFACE AREA m²/Gm	PARTICLE SIZE DISTRIBUTION (< X m, WT %) .2	.4	.6	1	4	6	20	40	75
411H, CR125, HPAl$_2$O$_3$	0.12	1.569	43.5	99.99	115	100								
666L, CR1, HPAl$_2$O$_3$	0.70	1.578	39.7	99.99	1		8	18	40	60	100			
4059, .1%C$_r$, CR125, HPAl$_2$O$_3$	0.12	1.932	52.6	99.99	115	100								
4060, .1%C$_r$, CR125, HPAl$_2$O$_3$	0.12	1.529	41.7	99.99	115	100								
4061, .01%C$_r$, CR125, HPAl$_2$O$_3$	0.12	1.577	43.0	99.99	115	100								
STANDARD Al$_2$O$_3$	1.2	2.234	55.9	99.98	0.5							40	80	100
STANDARD MgO	1.4	2.772	77.4	99.98	0.5							40	80	100
907, HP MgO	0.26	1.809	50.3	99.97	30				40	90	100			
6655 HP CORDIERITE	0.81	1.567	54.6	99.94	3				14	50	100			
6986 HP MULLITE	0.60	1.560	49.5	99.20	2				24	90	100			
HP DIAMOND	0.35	2.051	58.4	99.99	1	60	80	100						

NOTE: HP = High Purity

4.3.1 PART 1. EXPERIMENTAL CONSIDERATIONS

As mentioned earlier, there was a significant change in the scope of the planned research early in the Phase I project to include temperature as a test variable. In the Phase I proposal two irradiation facilities were mentioned as possible sources of the ionizing flux necessary for this study, namely, the High Flux Beam Reactor at Brookhaven National Laboratory, and the intense Gamma Source at the Oak Ridge National Laboratory. However, neither of these facilities could provide the appropriate temperature control required given the financial constraints of the Phase 1. In order to include temperature as a variable, an accelerator based source of ionizing radiation was considered as the best option. This had two major consequences. Firstly, the study of spinel insulation was postponed to Phase 2 to defray the unbudgeted $8,200 in added costs for the accelerator time. The second consequence was a reduction in the maximum achievable dose rate. The data for the mineral insulated coils were obtained up to a maximum dose rate 42 Gy/s, which is approximately two orders of magnitude below application dose rates such as the ITER first wall. However, through use of the accelerator it was possible to obtain data points in the range of 0.7 to 42 Gy/sec. As seen in Figure 2, the RIC phenomenon is generally directly proportional to dose rate which would allow straightforward extrapolation of our data into higher dose rate regimes. The data for the mineral insulated coils (given at the end of this section) also demonstrated linearity with dose rate, supporting this assumption.

The Gaertner linear accelerator at Rensselaer was chosen as the source of ionizing radiation. This facility provided an intense source of very high energy electrons (approx. 60 MeV) which were stopped in a water cooled tantalum target. Bremsstrahlung radiation (X-Rays) were produced in the electron-target interaction yielding a conical spread in radiation intensity along the original axis direction of the electrons. Prior to and following the sample irradiation, the dose rate was mapped using thermal luminescent dosimeters (TLDs). Results of this mapping are shown in Figures 7a and 7b. Figure 7a gives the absorbed dose in Grays per second as a function of the distance from the target. It is seen that there is a rapid drop-off in dose rate from over 150 Gy/s (three inches from the target) to a relatively flat region 25 inches from the target. As the Bremsstrahlung radiation is produced in a conical pattern it is equally important to know the dose rate dependence radially from the beam axis. This is shown in Figure 7b. From this figure it is seen that at 12 inches from the target there is a relatively flat region at least two inches in diameter. As will be mentioned shortly the coiled MI test sample was 2 inches in diameter and was therefore in the "flat" region.

Results being reported here are for the first iteration in testing which includes all alumina, mullite, cordierite and diamond cables. While all processing fabrication optimization was carried out the irradiation testing of MgO cables are scheduled for the second irradiation iteration. All cables were pulled through a 0.635 cm OD stainless steel tube and helically coiled around a mandrill. The total length of the coil was approximately 12 cm with a coil diameter of 5 cm. At either end of the coil the stainless steel tubing was bent in a direction radial to the helical axis. The coil was irradiated with the helical axis along the beam axis. The total length of cable in the irradiation field was approximately 300 cm.

The coil was irradiated inside a tube furnace under an atmosphere of flowing nitrogen. Temperature was monitored with two calibrated type-K thermocouples utilizing a Microstar controller to regulate furnace temperature. A five minute soak time was allowed following each increase in temperature to allow a steady-state temperature to be reached in the coil.

A program was written on LabView™ software to control a Keithley model 230 DC power supply and a model 236 source measure unit which measured the coil leakage current. The voltage was applied to the center conductor of the cables. For each cable a sweep from -100 to +100V was taken to confirm ohmic behavior of the cables and to yield to an accurate value of cable resistance. An appropriate settling time required to eliminate error due to cable capacitance was determined and used. A typical example of the raw data is shown in Figure 7c. In this figure the induced leakage current is shown as a function of applied voltage and radiation dose rate. It is seen that in the unirradiated as well as irradiated state this cable was ohmic in nature, as was typical of all cables in this study. Data on resistivity of the insulating material was obtained using the equation:

$$\sigma=(I/V)*\ln(Ro/Ri)/(2\pi L)$$

where I/V is the slope of the line fitted to the generated data (e.g. Figure 7C), Ri is the radius of the inner conductor, and Ro is the outer radius of the insulating material. L is the total length of cable being measured (300 cm).

4.3.2 PART 2. EFFECTS OF TEMPERATURE

The effect of temperature (in the absence of a radiation field) is shown in Figure 8. Temperatures of approximately 100, 300, 450, 600 and 750°C were chosen. As a first observation, it should be noted that near 100°C the cables had a very low conductivity and yielded currents near 10^{-11} A, which was close to the resolution limit of the electronics. However, it is seen that at these low temperatures several materials are as attractive as the standard MgO and Al_2O_3 typically used in mineral insulated cables with little difference between the standard and high purity Al_2O_3. As the temperature is increased above 100°C a significant difference in conductivities of these materials occurs. At 300°C both mullite and cordierite increase by more than three orders of magnitude over their 100°C values. Also the conductivity of the high purity CR125 Al_2O_3 powder has a very low value near 100°C. The standard Al_2O_3 exhibits a much larger increase in conductivity between 100 and 300°C. Interestingly the absolute difference between the standard and high purity materials is well over an order of magnitude at elevated temperatures. Also of interest in this figure is that the Type 1B synthetic diamond, which should have a very low intrinsic conductivity (10^{-14} S/m), remains relatively low with elevated temperatures and is comparable at the alumina and magnesium oxide cables.

Figure 9 gives the conductivity dependence of the chromia doped alumina as a function of temperature. As will be discussed later, this material proved very difficult to study because of the high "baseline" conductivity of the doped material. In this figure, both the 0.01 and 0.1% chromia doped powder showed a conductivity significantly higher than the CR125 (undoped) Al_2O_3 (although still well below Phase I acceptance criteria of 10^{-7} S/m). This baseline conductivity was seen to be a constant with temperature until the thermally enhanced conductivity began to dominate above 450°C, at which point all three powders had virtually identical conductivities. This baseline conductivity is not understood, and analysis of the Cr_2O_3 doped alumina coils as well as other controlled experiments is considered an important part of the Phase II research in order to understand this conduction mechanism.

4.3.3 PART 3 EFFECTS OF IRRADIATION

By varying the distance from the tantalum accelerator target the dose rate applied to the cables was varied to give dose rates of 0.7, 7.0 and 42 Gy/s. A relative comparison of the radiation induced conductivities of

the candidate materials is given in Figure 10 for data generated near 100°C. The RIC was easily separated from any thermal component at this temperature and remained unchanged at the higher temperatures. The diamond insulated cable suffered the highest RIC of those materials considered. By comparison of the three alumina powders studied, it is interesting to note a large difference in RIC behavior, with the standard alumina exhibiting more than an order of magnitude higher RIC than the high purity CR125 alumina. Extrapolation of the results of Figure 10 to the high dose rates expected for these cable applications is given in the following section.

Finally, the chromia doped CR125 alumina did not show observable RIC and the effect of the doping on the RIC could therefore not be determined. This was due to the excessively high baseline conductivity of the chromia doped alumina cables. However, it is possible that the chromia doping has substantially affected the RIC of this cable and it is felt that the concept should be carried into Phase II.

4.3.4 PART 4 DISCUSSION AND ASSESSMENT OF RESULTS

As mentioned earlier, conductivity of mineral insulated cables can be separated into three components: 1) RIC, 2) Thermally Excited Conductivity and 3) Baseline conductivity.

$$(1) \qquad \sigma_{tol} = \sigma_{RIC} + \sigma_{th} + \sigma_{base}$$

Two examples of the separability of these components are shown in Figures 11 and 12. Figure 11 shows data from the CR125 high purity Al_2O_3, cable as a function of irradiation temperature, both during irradiation and without irradiation. The graph plots the thermal component of the conductivity, which for monolithic alumina and other ceramics has been shown (Ref. 14) to follow the relation:

$$(2) \qquad \sigma_{th} = Ae^{-(E/kT)}$$

where A is a constant, k is Boltzmann's constant, E is the activation energy and T is the absolute temperature. The RIC component of conductivity (see equation (1)) is found by subtracting the conductivity in the absence of the ionizing radiation from the conductivity during the irradiation (i.e. beam on - beam off). As expected, the RIC component is independent of temperature at least to 450°C, after which point the thermal contribution to conductivity was so great the RIC component could not be measured. In Figure 11 the open squares at 600 and 750°C are assumed values of RIC, not measured data.

The additional complication of a high baseline conductivity is demonstrated in Figure 12 for the CR1 high purity alumina. In this case a baseline conductivity was measured in the absence of radiation as a function of temperature and was seen to remain constant to at least 450°C at which point the thermally stimulated current began to dominate (clearly seen above 600°C in the figure). The RIC component at this irradiation level was comparable to the baseline conductivity and therefore easily differentiable over all temperatures measured. As with the previous figure the RIC was seen to remain constant with temperature.

It should be noted that the data generated in this study cannot determine the mechanism behind the baseline conductivity. Possible mechanisms could include one or more of the following:

- bulk conduction in the powder grains

- surface conduction over the powder grains

- conduction through the argon fill gas

While none of these mechanisms can be ruled out, it seems unlikely that the baseline conductivity as seen in CR1 Al_2O_3, and chromia doped CR125 Al_2O_3 could be caused by bulk conduction as this would show some temperature dependence, which did not occur.

From the previous two sections it is clear that the selection of the appropriate mineral insulation for a cable used in a radiation environment will not only have to take into account the irradiation level expected in the application, but also the application temperature. Using the ITER diagnostic probe as an example, the expected application temperature is somewhere between 300 and 600°C, and the maximum tolerable conductivity is expected to be 10^{-7} S/m. This value of 10^{-7} S/m may be further reduced as further ITER design and magnetic probe performance information becomes available.

A relative comparison of the RIC in the materials studied which has been extrapolated from the data in Figure 10 to and dose level of 10^4 Gy/s, is given in Table 4. Based on this data and the data from Figure 8, four materials studied in this Phase I work can be eliminated from further consideration. Referring again to Figure 8, both cordierite and mullite have thermally induced currents greater than the acceptance criteria (near 600°C) and can be dropped, even though they have very low RIC. Conversely, diamond and standard alumina, which have acceptable thermally stimulated conductivity, have unacceptably high RIC and can be dropped since their conductivity extrapolated at 10^4 Gy/s is 10^{-7} S/m.

However, two insulating cables, the CR1 Al_2O_3, and CR125 Al_2O_3 appear quite attractive. Figures 13 and 14 give the effect of dose rate and temperature on these cables. It is seen that the conductivity at low temperatures (where the thermal component is negligible) is increased with dose rate as expected. Due to the relatively high baseline conductivity of the CR1 Al_2O_3, this material has a conductivity higher than that of the CR125 Al_2O_3 at temperature below approximately 450°C. However, as the temperature is increased, the greater thermal component to conductivity of the CR125 Al_2O_3, dominates its conductivity giving it substantially higher conductivity than the CR1 Al_2O_3 at elevated temperatures.

The primary goal of this Phase I research of achieving a cable with conductivity $<1 \times 10^{-7}$ S/m at a dose rate of 10^4 Gy/s, is addressed in Figure 15. This figure is identical to Figure 2 with the addition of the CRI and CR125 Al_2O_3, mineral insulated cables. The added cable data corresponds to a maximum temperature of 450°C for the CR125 and 600°C for the CR1. One unexplainable observation from Figure 15 is that the slope of the conductivity-vs-dose rate curves of the alumina cables for the dose rates studied in Phase I is less than the expected linear behavior seen in previous work with monolithic ceramics. The behavior of these mineral insulated cables is a sublinear, nearly square root dependence. In order to extrapolate the effect of increasing the dose rate to 10^4 Gy/s two assumptions can be made. The first is that the sublinear behavior will continue along the same path as shown by the solid lines in Figure 15. In this case the extrapolated conductivity would be $<10^{-9}$ S/m, or two -orders of magnitude below the Phase I goal. A more conservative approach would be to assume that for dose rates greater than the upper dose rate of this study (42 Gy/s) that the cables begin to behave linearly, i.e. have the same slope as the monolithic materials. This assumption is also depicted by dotted lines in Figure 15 and yields an extrapolated conductivity of $<10^{-8}$ S/m, or more than one order of magnitude lower conductivity than the Phase I goal. While either of these assumptions demonstrate promising performance, higher dose rate testing as well as the in-core tests proposed in Phase II are necessary.

Based on the number of possible variables which potentially contribute to the conductivity of the materials studied in this work, it is difficult to draw precise conclusions as to what form of a particular material type (e.g. large particle size alumina), or what process parameters are best. Among a family of materials indicators are that high purity powders with a small particle diameter give the best performance. This supposition will be carried into the Phase II study and will be emphasized. However, Phase II will not be limited to those parameters.

4.4 TASK 4: MECHANICAL ASSESSMENT

Task Statement. Determine if the candidate cables could be formed into complex shapes needed for sensors and diagnostics. The example used was the tightly wound (helical) magnetic probe sensor. Once formed, the cables were tested for electrical property degradation.

Results. Tests conducted under Task 2 were used to determine if winding the coaxial cables into the diagnostic configuration of approximately 3.8 cm diameter helical coils had any degrading effect on the material conductivity. Table 2 compares the room temperature insulation resistance (IR) before and after coiling. Of the eleven cables evaluated the IR remained the same on four, increased slightly on four, and decreased slightly on three. It thus can be concluded that winding the cables into helical shapes had no deleterious affect on insulation resistance.

Further supporting evidence for the lack of insulating property degradation was observed from the 50 meter coils purchased from DELTA M by General Atomics. These MgO cables were coiled into 1.7-cm diameter, 25-cm long helical coils for testing in the High Flux Beam Reactor. Insulating resistance was measured to be between 15 and 20 Gigaohms prior to and after coil forming.

5.0 SUMMARY AND CONCLUSIONS

The use of insulating cables for applications in high radiation fields has become problematic due to the breakdown in electrical properties of the insulating materials used. Generally, for applications with modest ionizing or displacive radiation fields the use of mineral insulated cables is required. In many nuclear applications, however, a sizeable immediate degradation occurs which can render components such as diagnostic probes useless. As example, magnetic diagnostics are of critical importance for the operation of tokamaks such as the International Thermonuclear Experimental Reactor (ITER) machine. Due to the enhanced gamma and neutron flux expected in the ITER machine, analysis has shown that sensor types proposed in the Conceptual Design Phase of ITER and by the ITER Joint Central Team are basically inadequate.

The purpose of this work was to develop improved mineral insulated cables with decreased and radiation induced electrical conductivity (RIC), specifically to develop a cable with conductivity $<1 \times 10^{-7}$ S/m at a dose rate of 10 Gy/s.

The research included: (1) selection of starting materials with low intrinsic RIC and (2) optimization of the processing parameters to develop viable low leakage cables for nuclear environments. Insulation materials selected included alumina, mullite, cordierite, and diamond. Candidate cables were irradiated at the Gaertner linear accelerator at Rensselaer Polytechnic Institute. Dose rates of 0.7, 7.0 and 42 Gy/s were obtained.

This Phase I effort demonstrated that mineral insulated coaxial cables, would meet the primary technical objective of <10-7 SIM at tokamak-relevant radiation cases with the appropriate selection of insulating material. Two alumina insulated cables had extrapolated conductivites of approximately 10^{-9} S/m at 10^4 Gy/s which is a dose rate typical of fission power systems, that expected for fusion machines such as ITER, and approximately one order of magnitude higher than many research accelerators. Additionally a fundamental knowledge of the mechanisms responsible for conduction in these cables was obtained and a technology base for fabrication of these cables was developed.

The primary potential application of the improved mineral insulated cable is for magnetic diagnostics for fusion reactor programs. Other applications include accelerators, commercial nuclear reactors, and Naval nuclear reactors.

6.0 REFERENCES

1. ITER Technical Meeting on Radiation Effects on In-Vessel Components, Garching, 15-19, Nov. 1993.
2. U.S. Home Team Report Task IVA-2. Prepared for the In Vessel Ancillaries Division ITER Joint Central Team, Garching, Germany. 18 March, 1994.
3. E.R . Hodgson and S. Clement. "The Effect of Iron on the Radiation Induced Conductivity in Gamma and Electron Irradiated Mgo,-' Radiation Effects, 97 (1985) pp 251.
4. R.W. Klaffky et al., Phys. Rev., B21 (1980) 3610.
5. G.P. Pells, Rad. Effects 97 (1986) 199.
6. V.M. Ivanov, et al., Inorganic Mater., 17 (1981) 1303.
7. E.R. Hodgson, Cryst. Latt. Def. Amorph. Mat., (18), 169 (1989).
8. E.R. Hodgson, J. Nucl. Mater., 179-181 (1991) 383.
9. E.R. Hodgson, J. Nucl. Mater., 191-194 (1992) 552.
10. G.P. Pells, J. Nucl. Mater., 184 (1001) 177.
11. T. Skikama, et al, J. Nucl. Mater., 191-194 (1992) 575.
12. E.H. Farnum, private comm. (LASREF irradiation of Al_2O_3).
13. E.R. Hodgson, Rad. Eff. Def. Solids, 119-121 (1991) 827.
14. L.L. Snead, D.P. White and S.J. Zinkle. "Investigation of Radiation Induced Electrical Degradation in Alumina Under ITER-Relevant Conditions," Accepted J. Nucl. Matter. 1995.

15. Walter H. Gitzen, editor. "Alumina as a Ceramic Material". The American Ceramic Society, Special Publication No. 4 (1970), pg. 76.

16. L.L. Snead, "Radiation Enhanced Conductivity in Silicon Carbide Materials," Fusion Reactor Materials Semiannual report, DOE/ER-0313, 1992.

17. L.L. Snead, "In-Core Measurement of DC Electrical Conductivity of Ceramics," Accepted, Journal of Nuclear Materials, 212-215 (1994), 1107.

TYPICAL SEMI RIGID COAXIAL PROBE

FIGURE 1

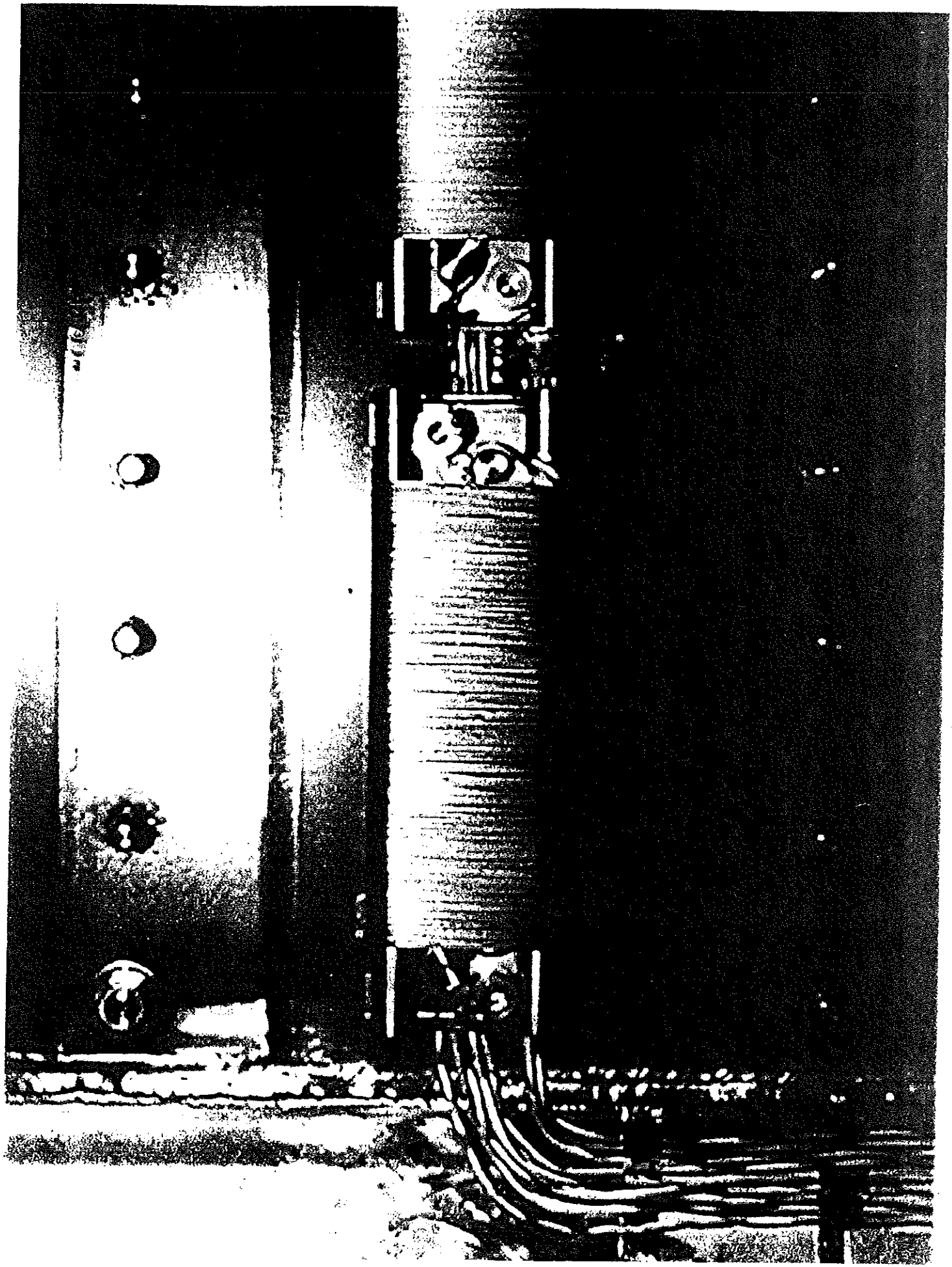

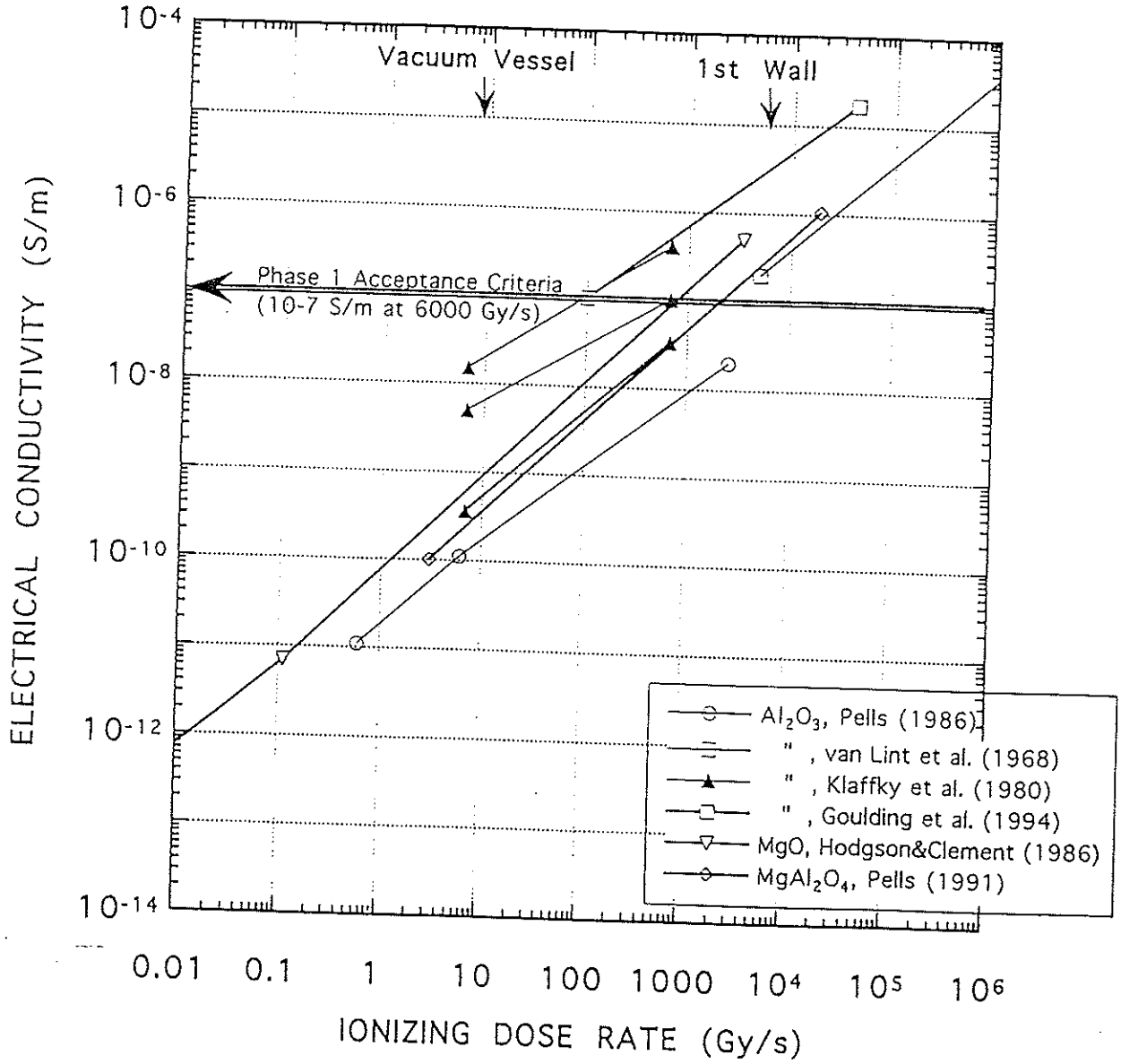

FIGURE 2

FIGURE 3

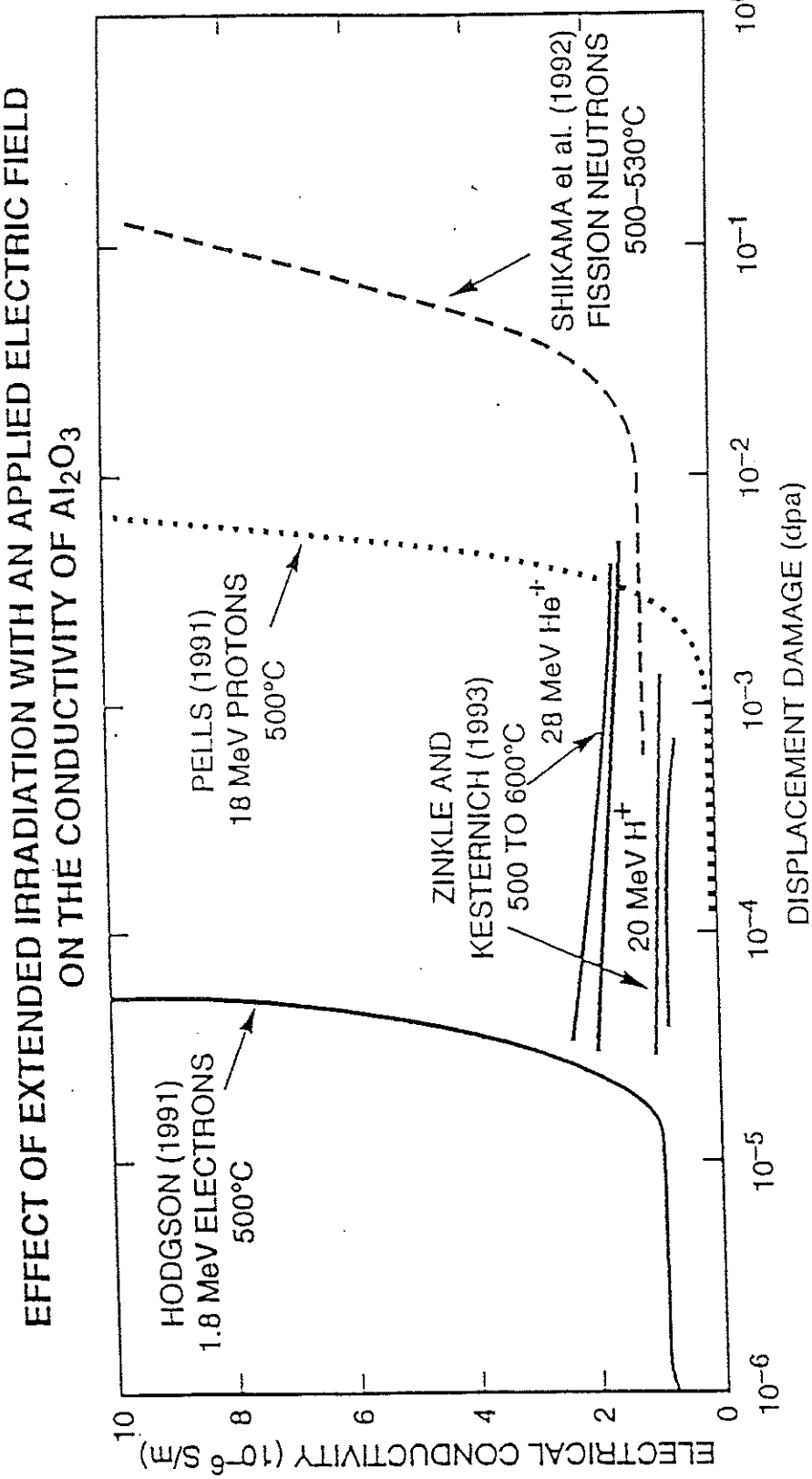

FIGURE 4a ALUMINA INSULATED COAXIAL CABLE

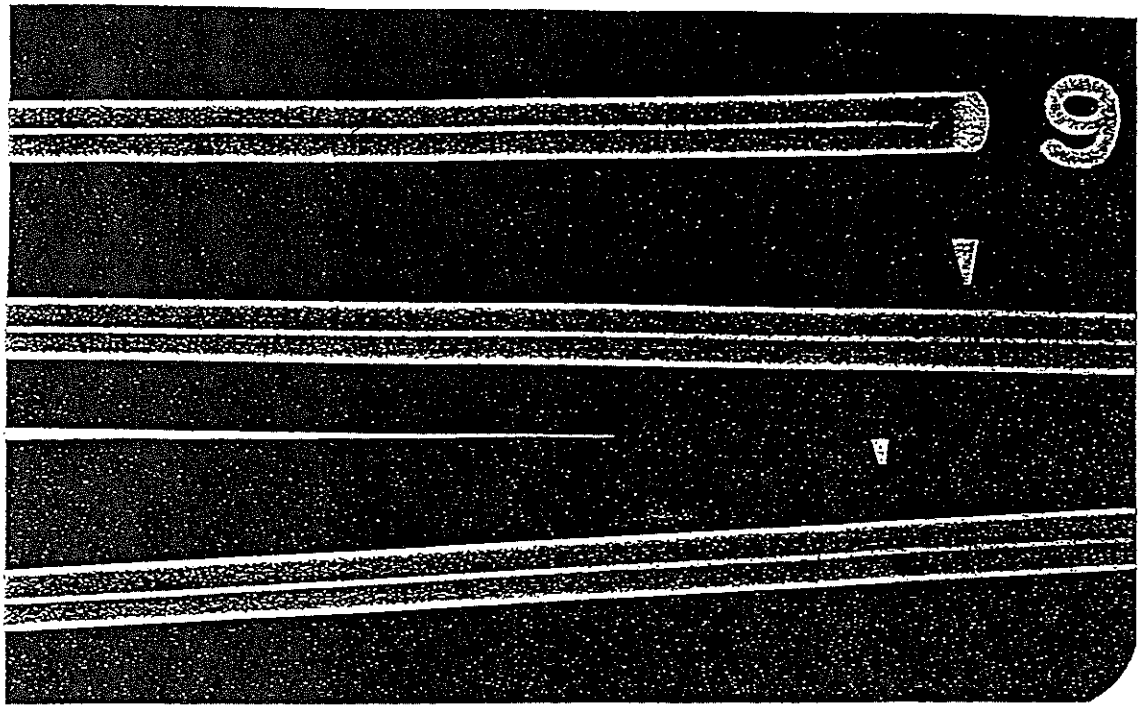

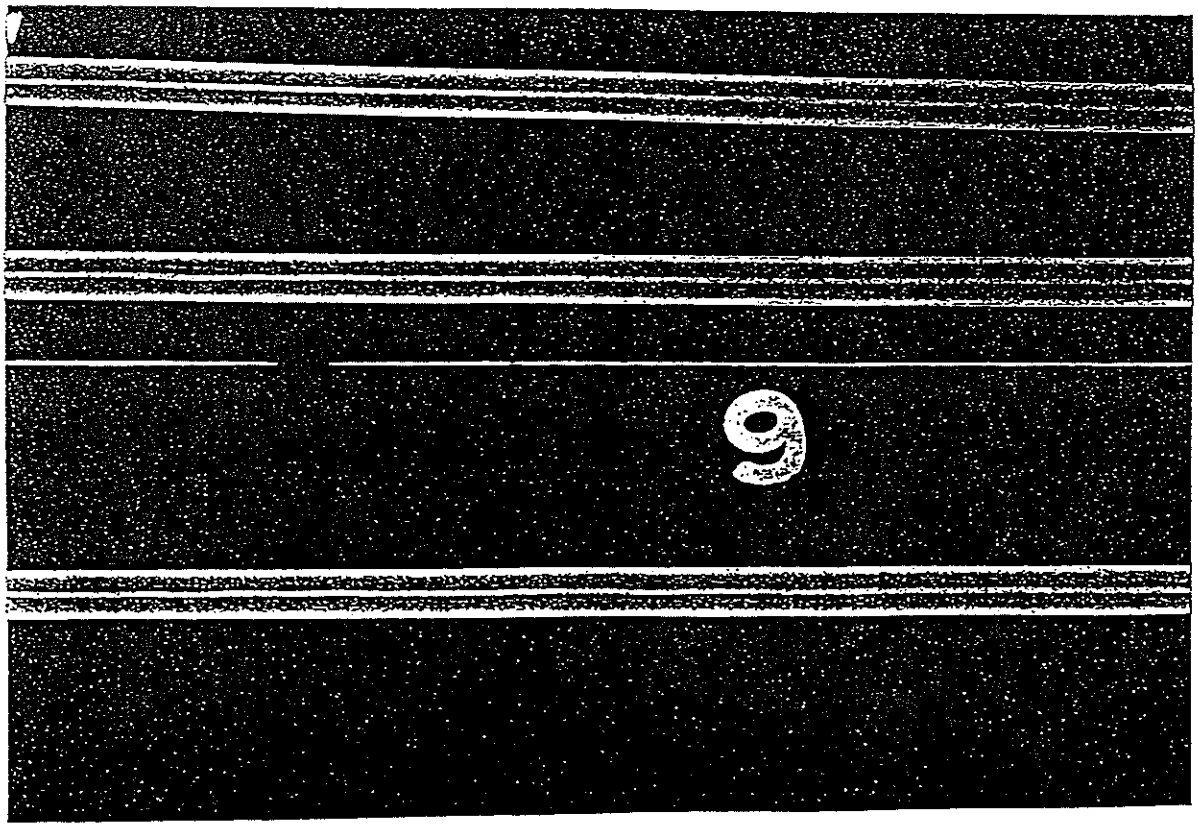

FIGURE 4b SILICA INSULATED COAXIAL CABLE

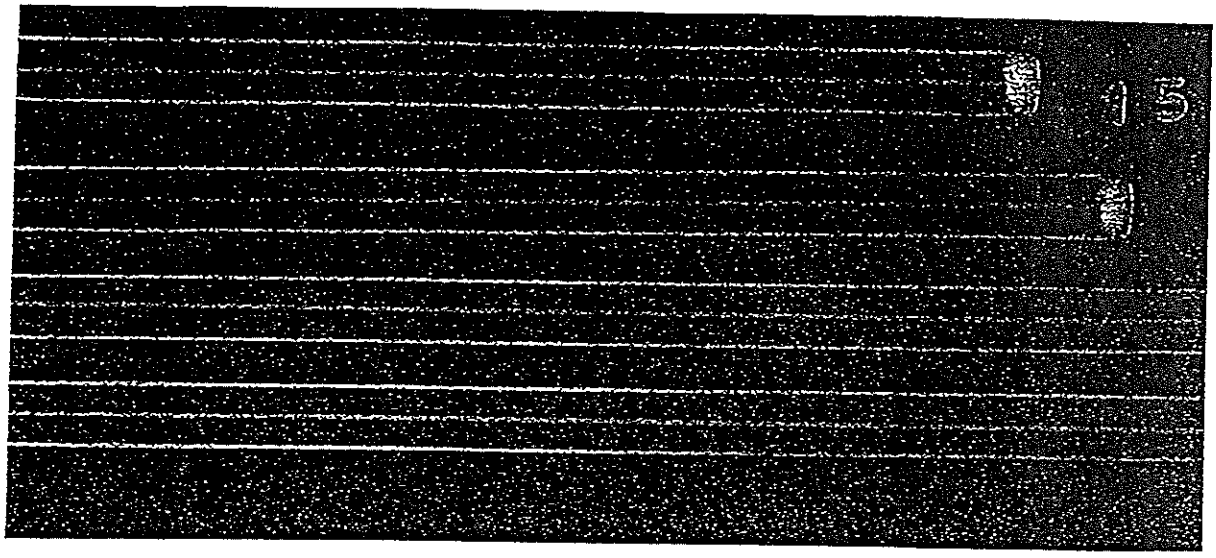

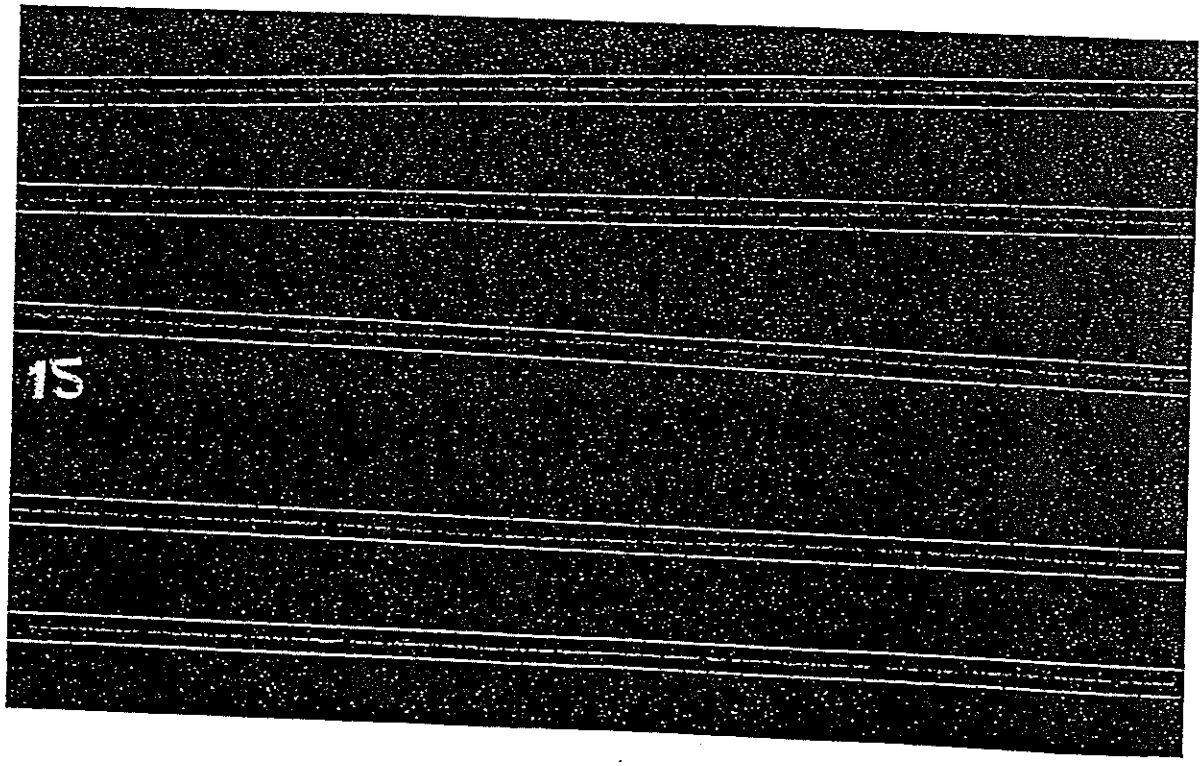

FIGURE 5A

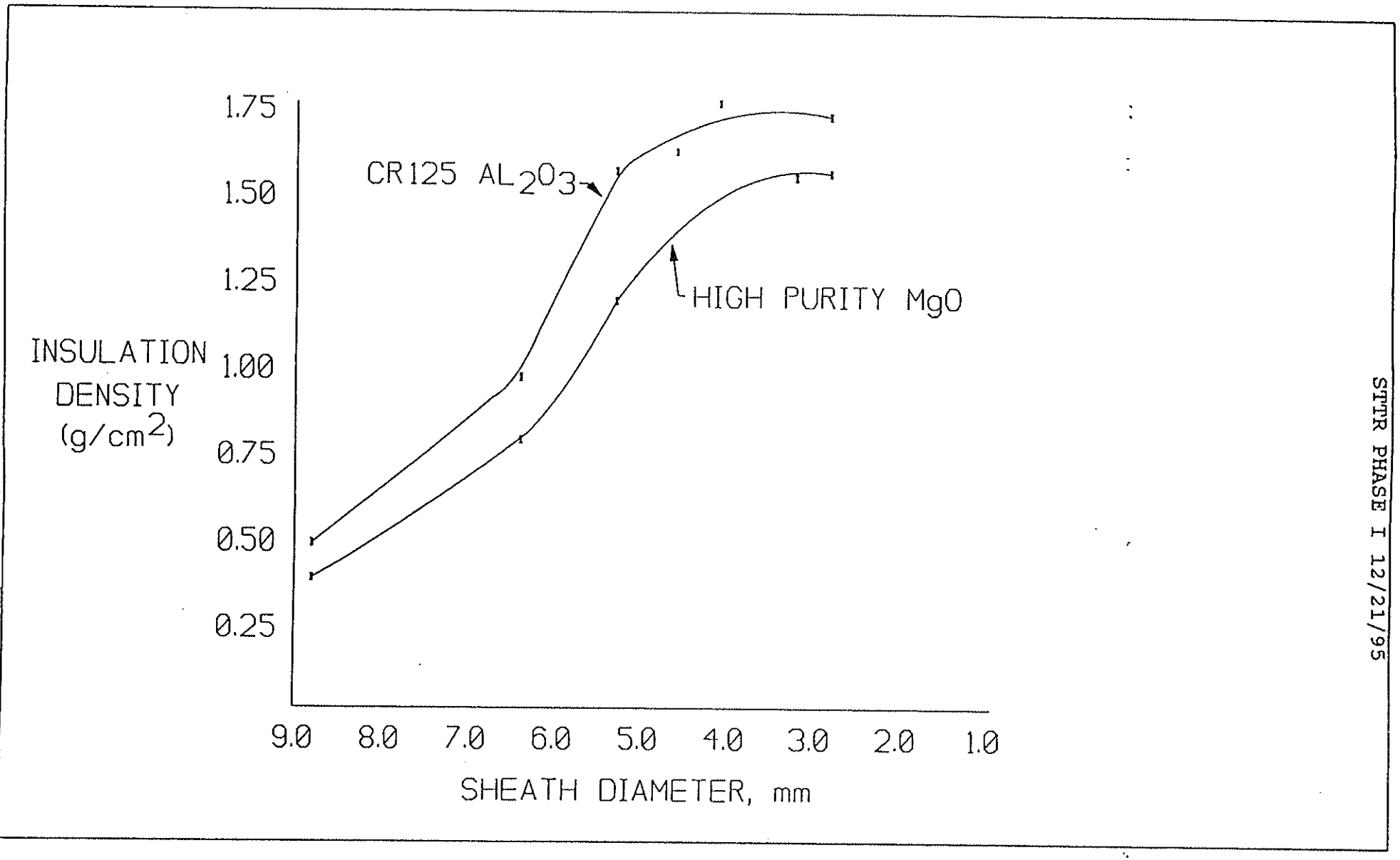

FIGURE 5: INSULATION DENSITY VS DIAMETER
VS DIAMETER FOR TWO SELECTED MATERIALS

FIGURE 5B

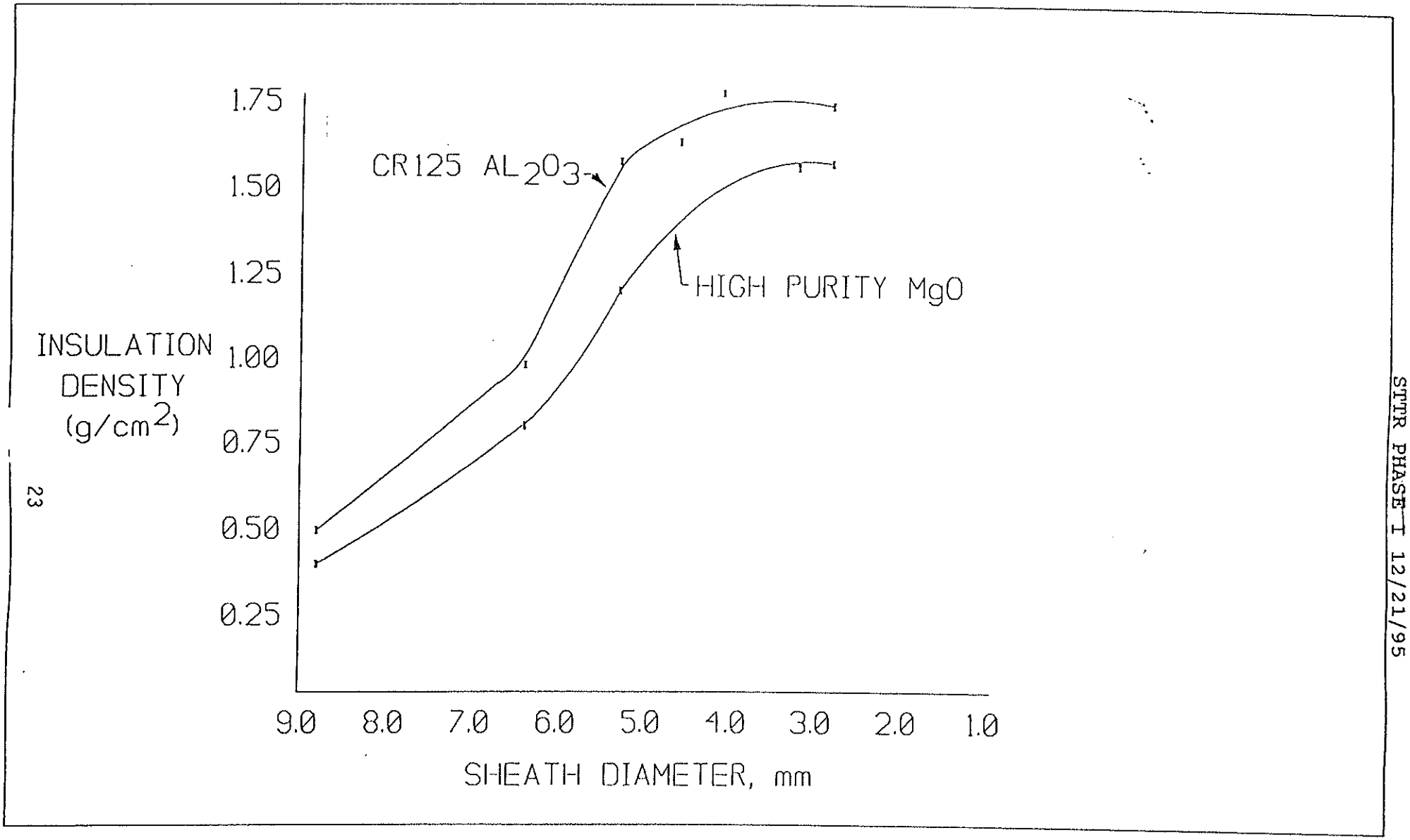

FIGURE 5: INSULATION DENSITY VS DIAMETER VS DIAMETER FOR TWO SELECTED MATERIALS

"PROTECTED CRADA INFORMATION"

FIGURE 6a Typical Micrograph of a Coaxial Cable

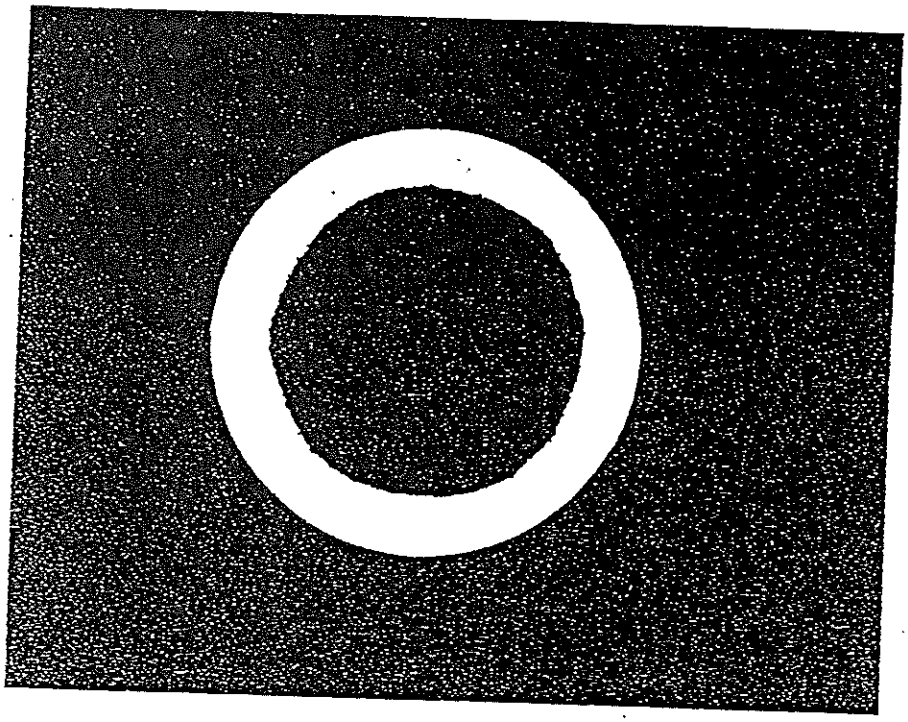

FIGURE 6b Coaxial Cable Showing Some Distortion to the Outer Conductor

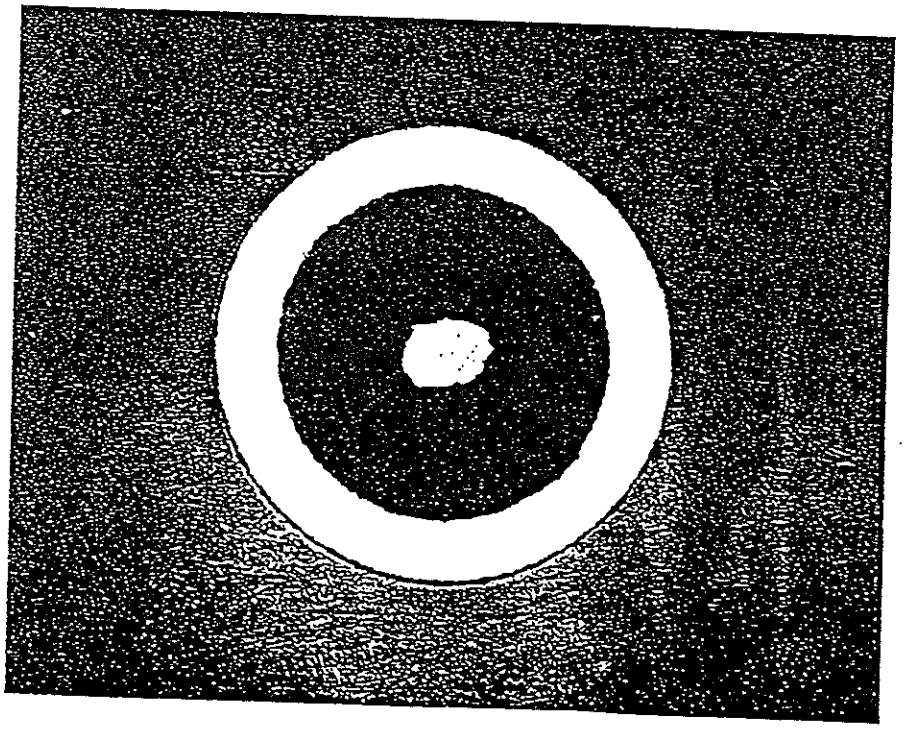

FIGURE 7a

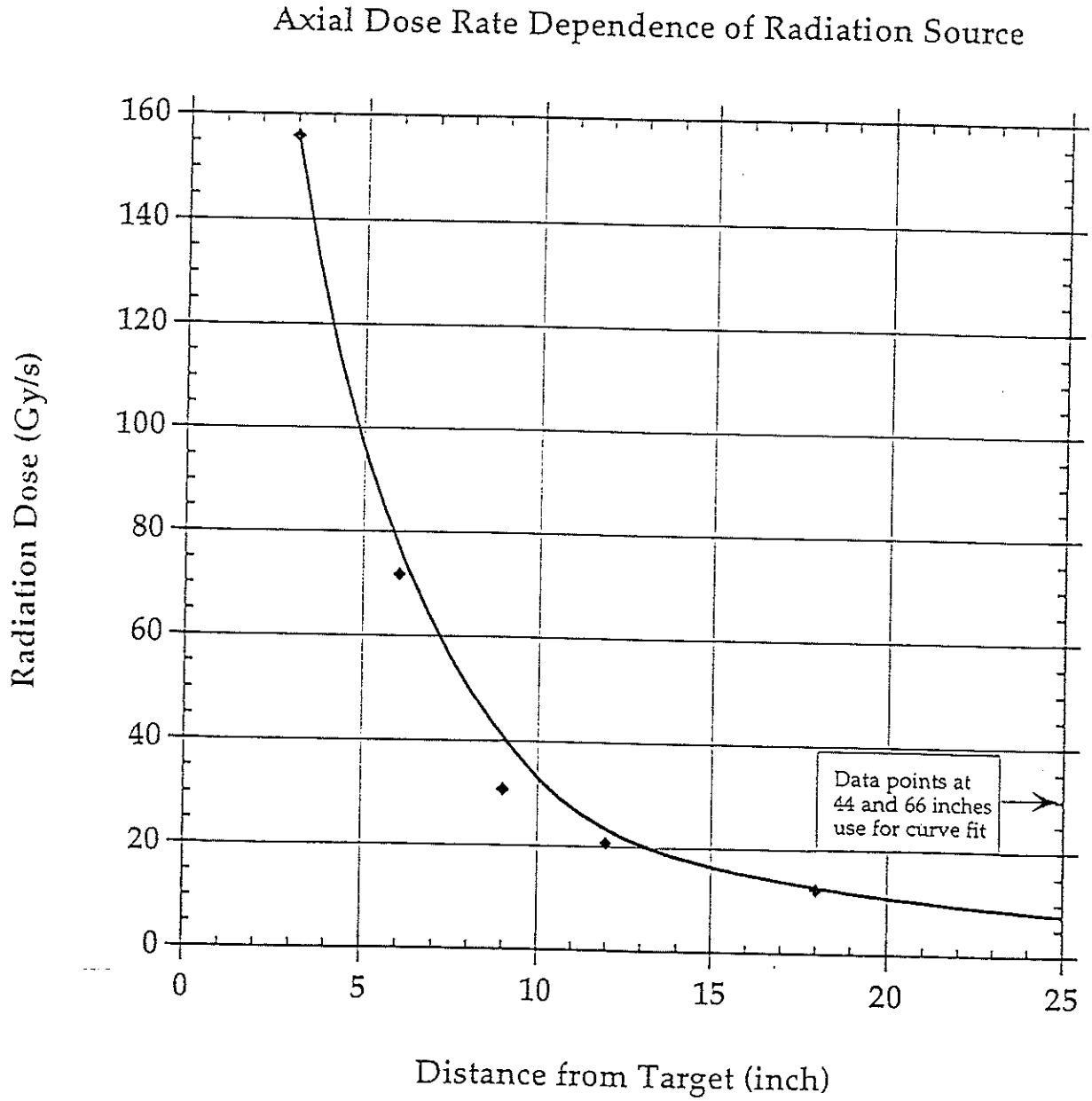

FIGURE 7b

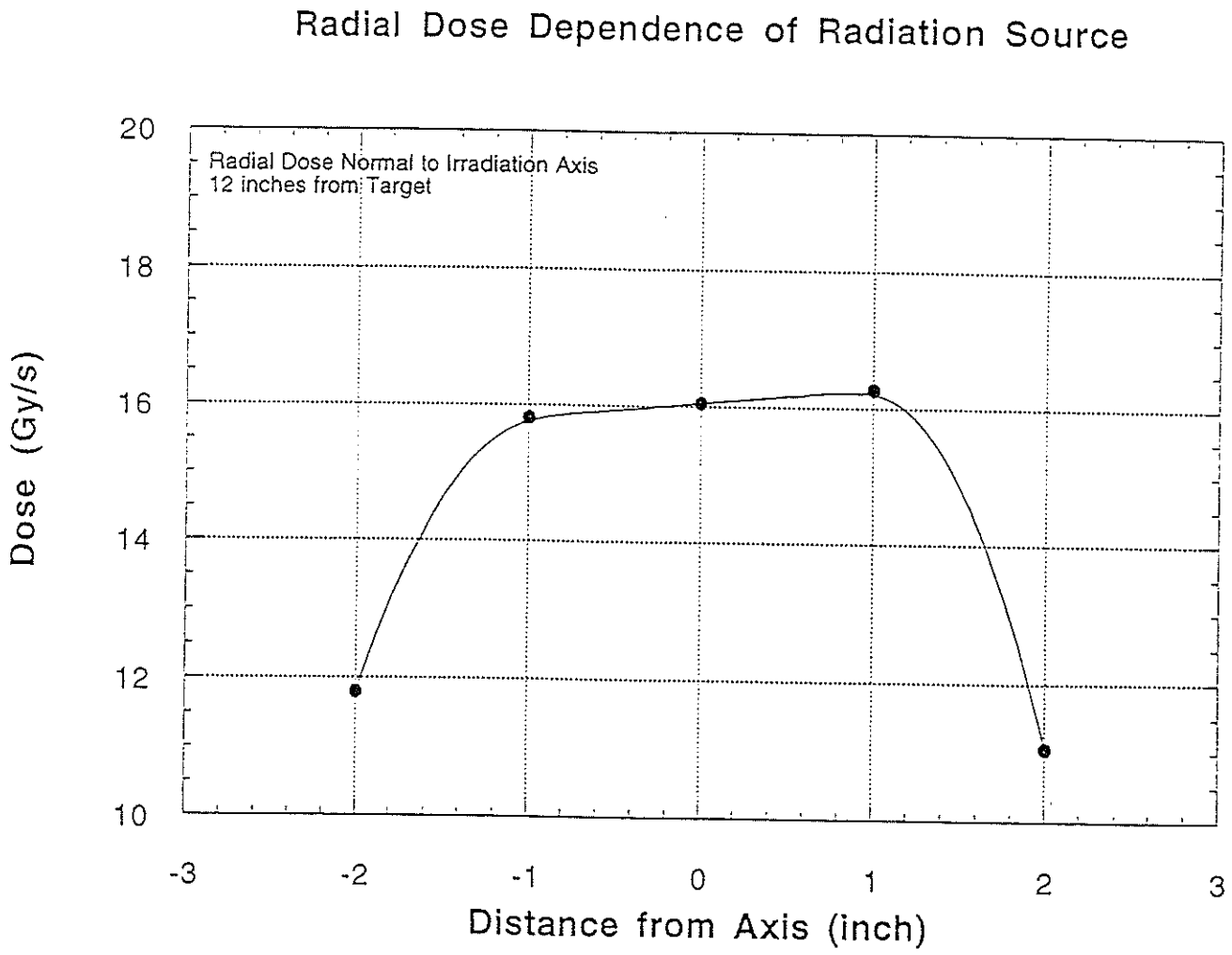

FIGURE 7c

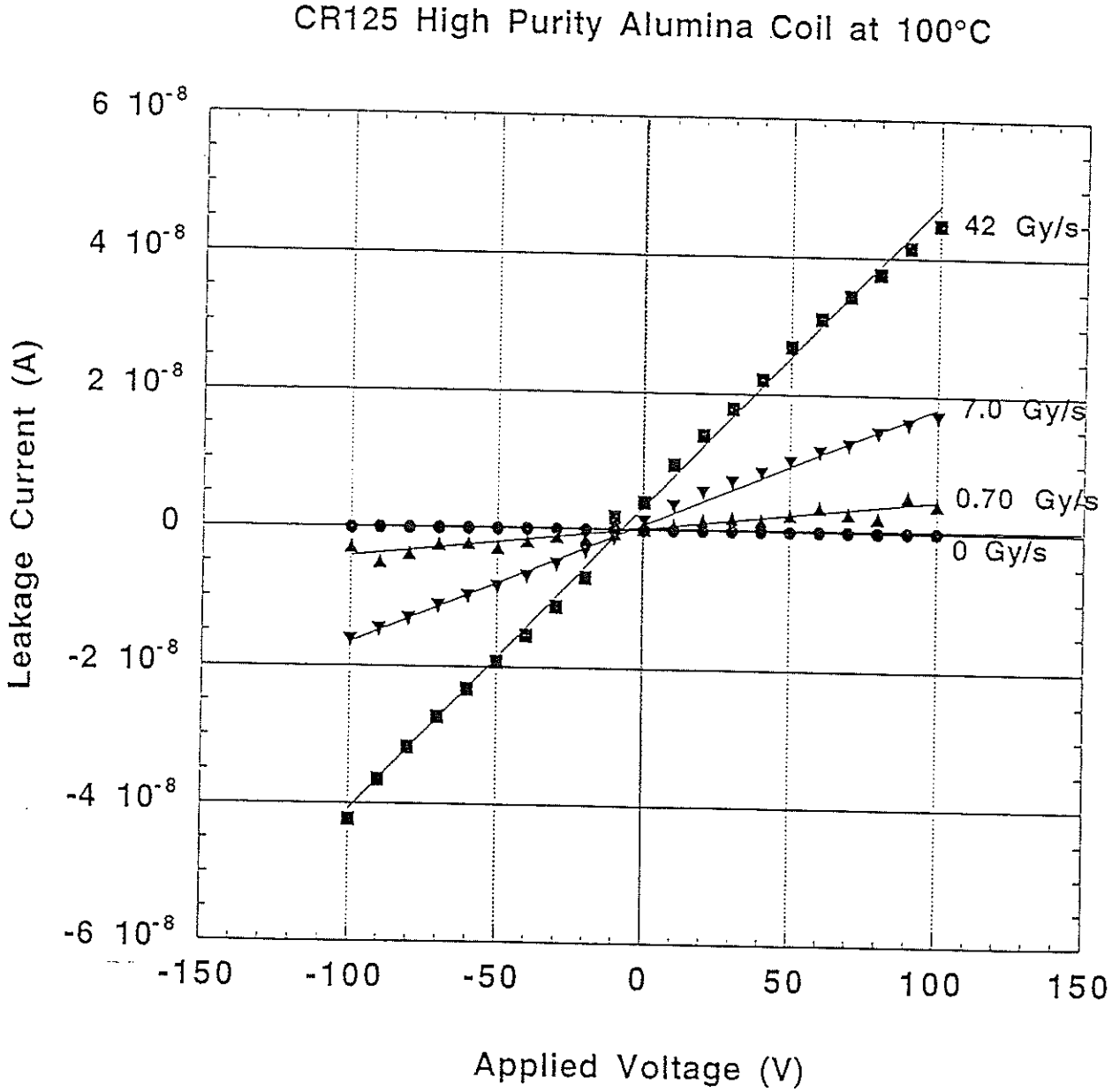

FIGURE 8

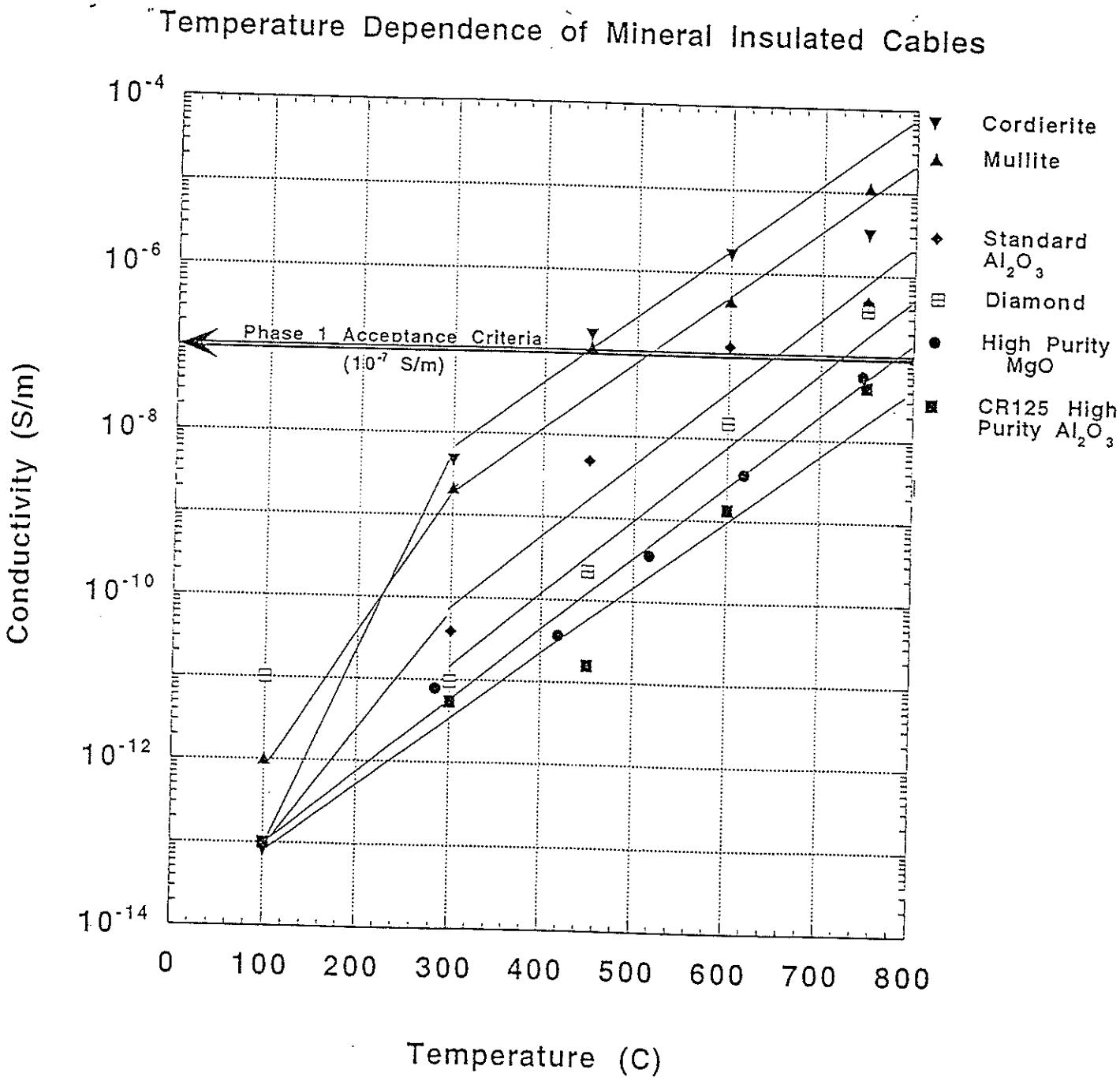

FIGURE 9

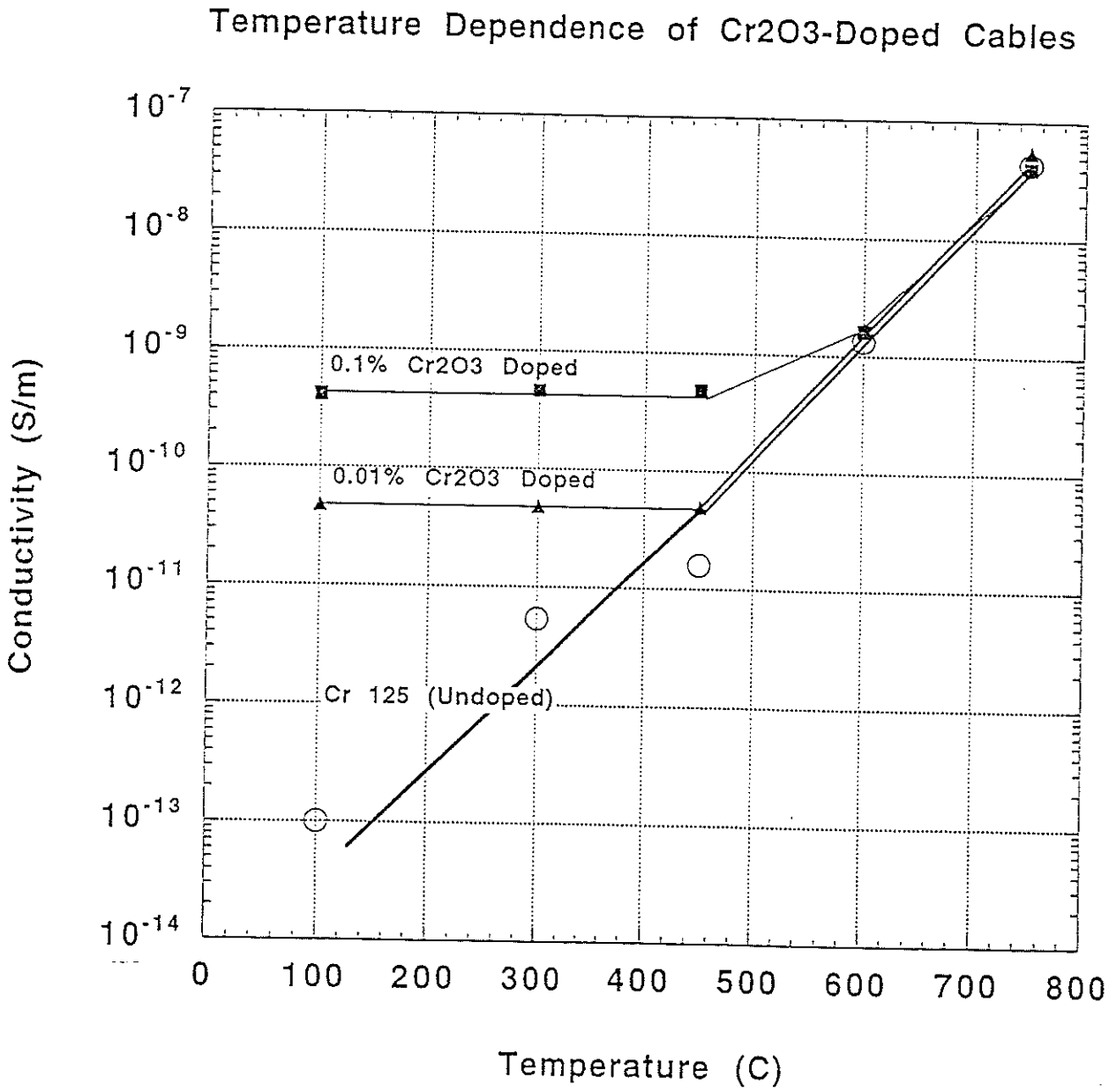

FIGURE 10

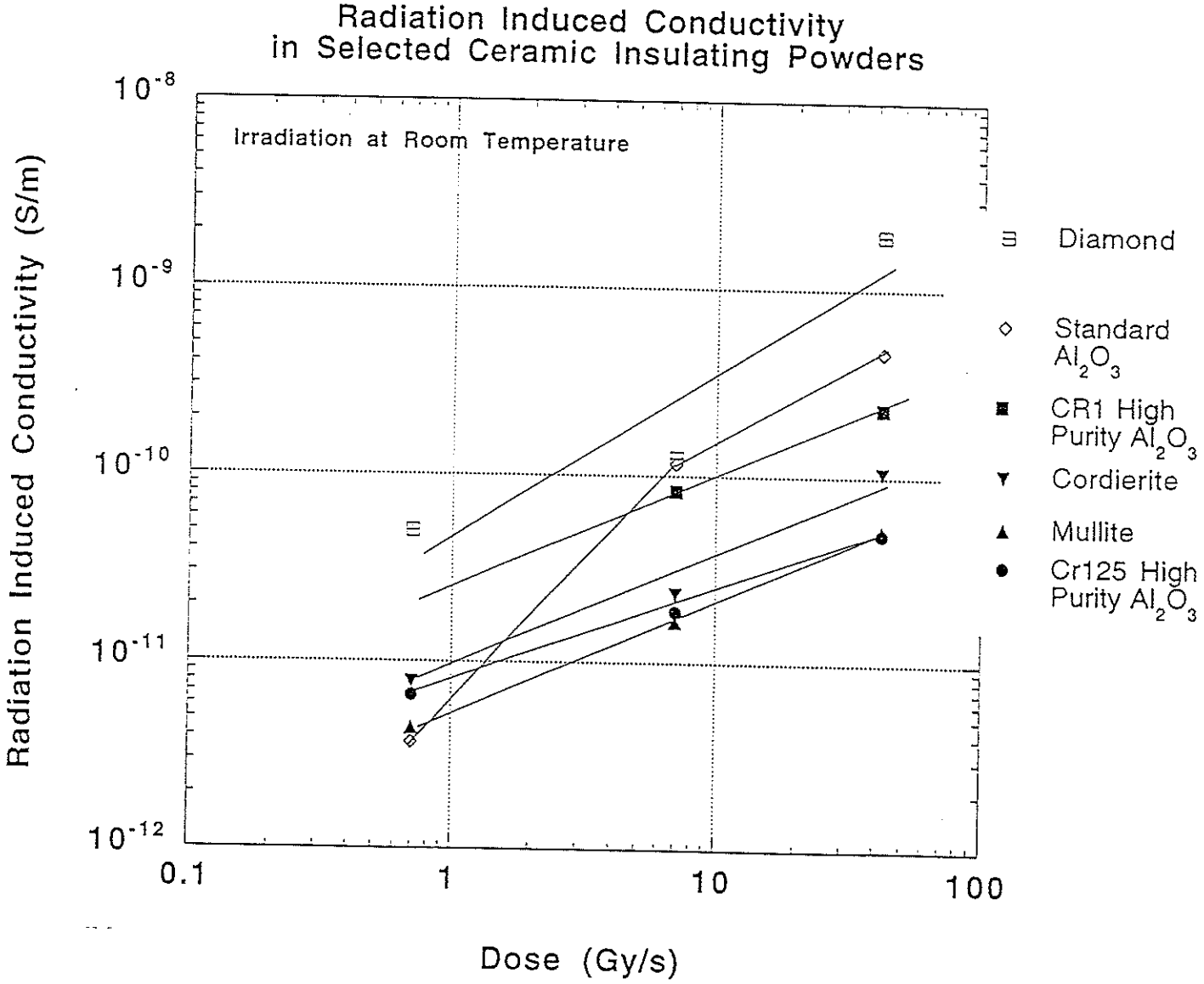

FIGURE 11

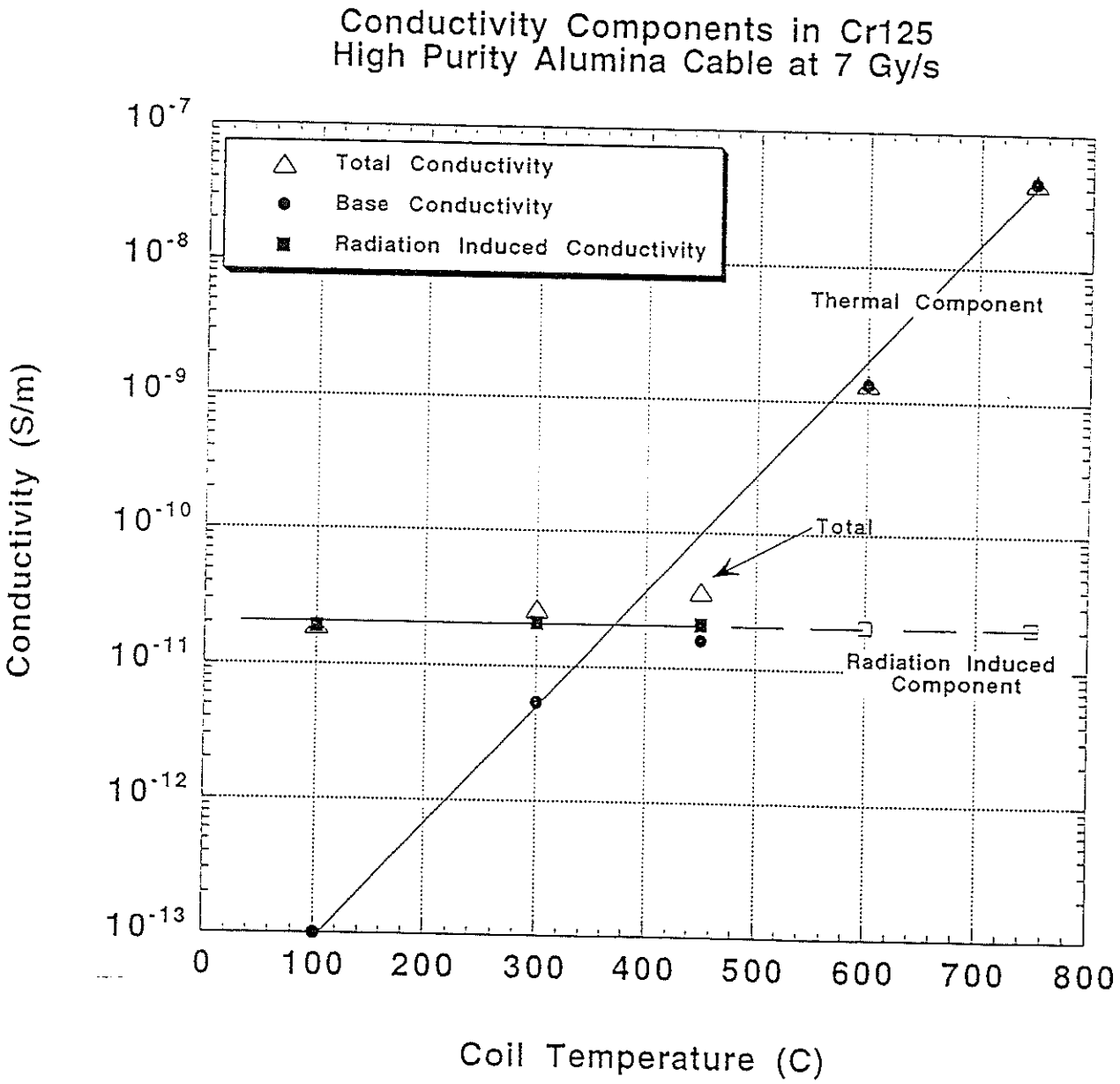

FIGURE 12

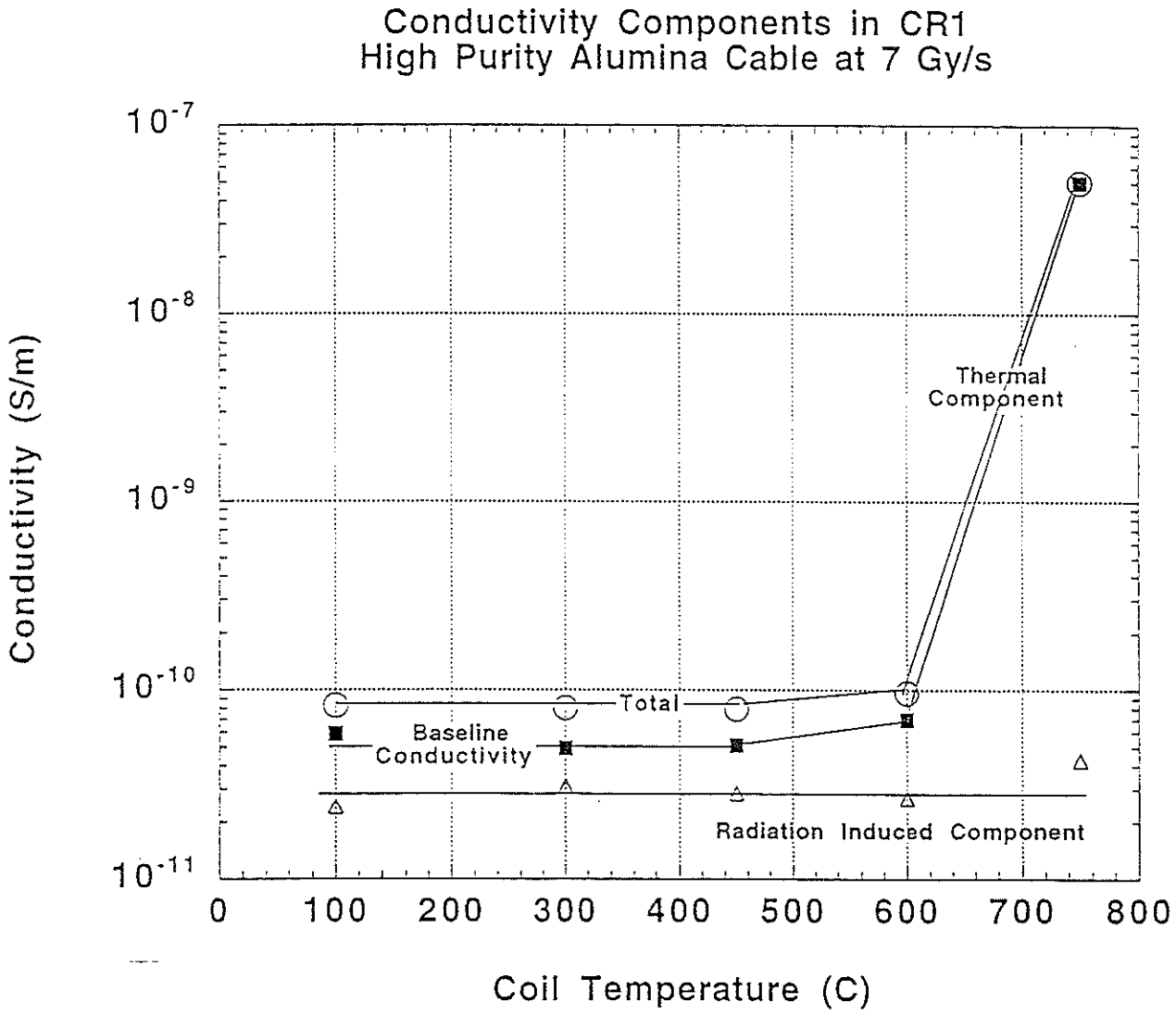

FIGURE 13

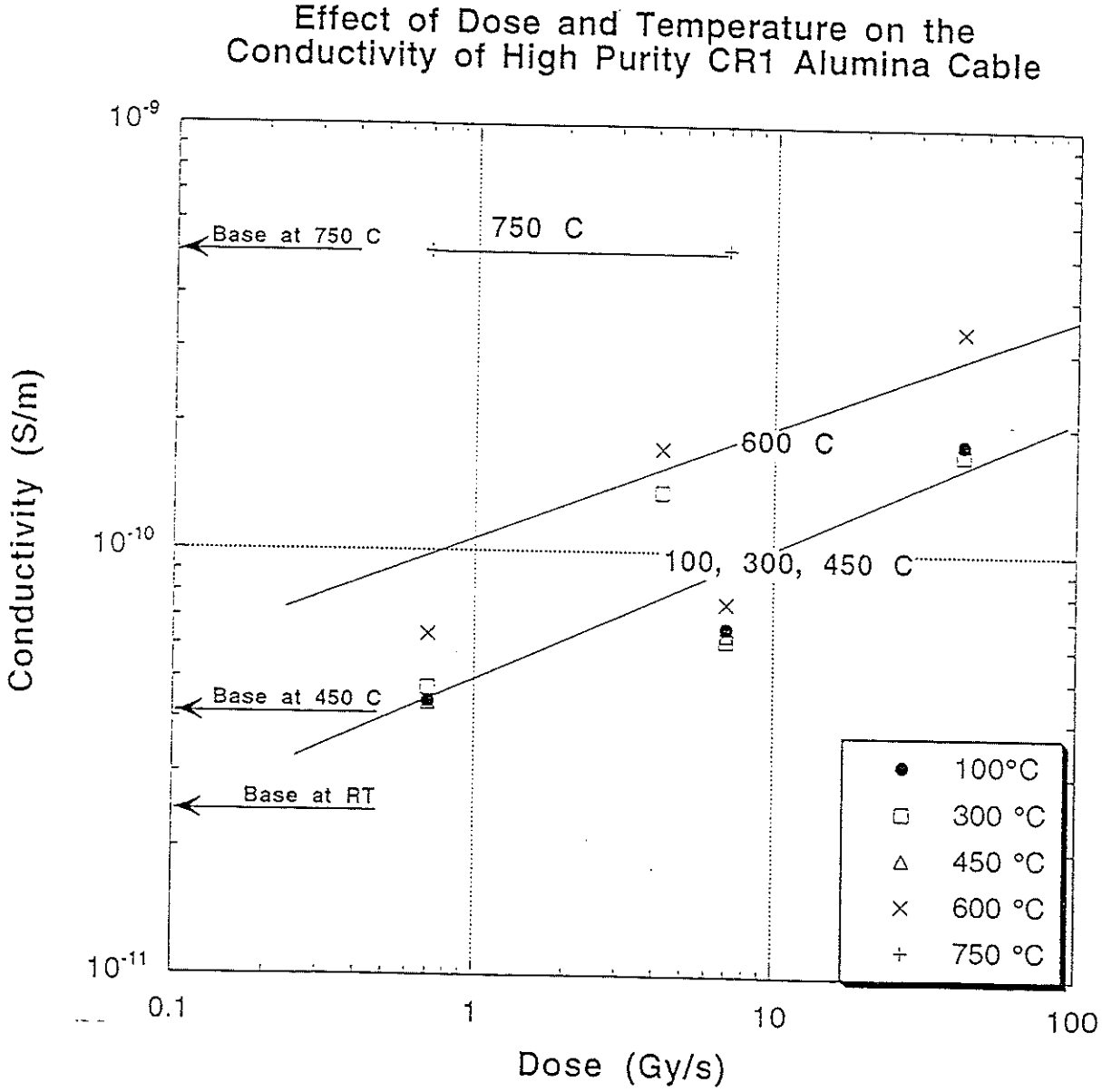

FIGURE 14

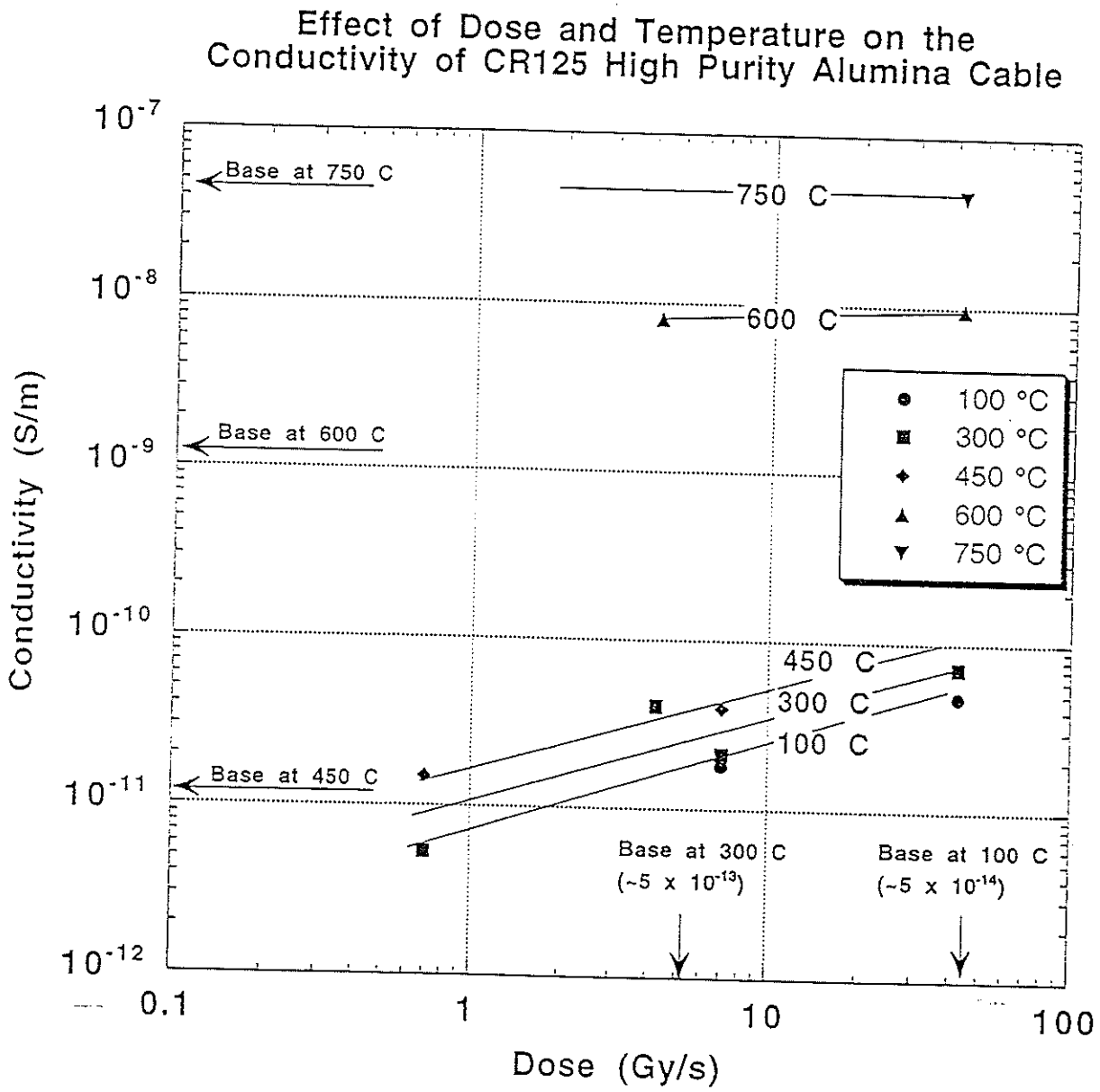

FIGURE 15

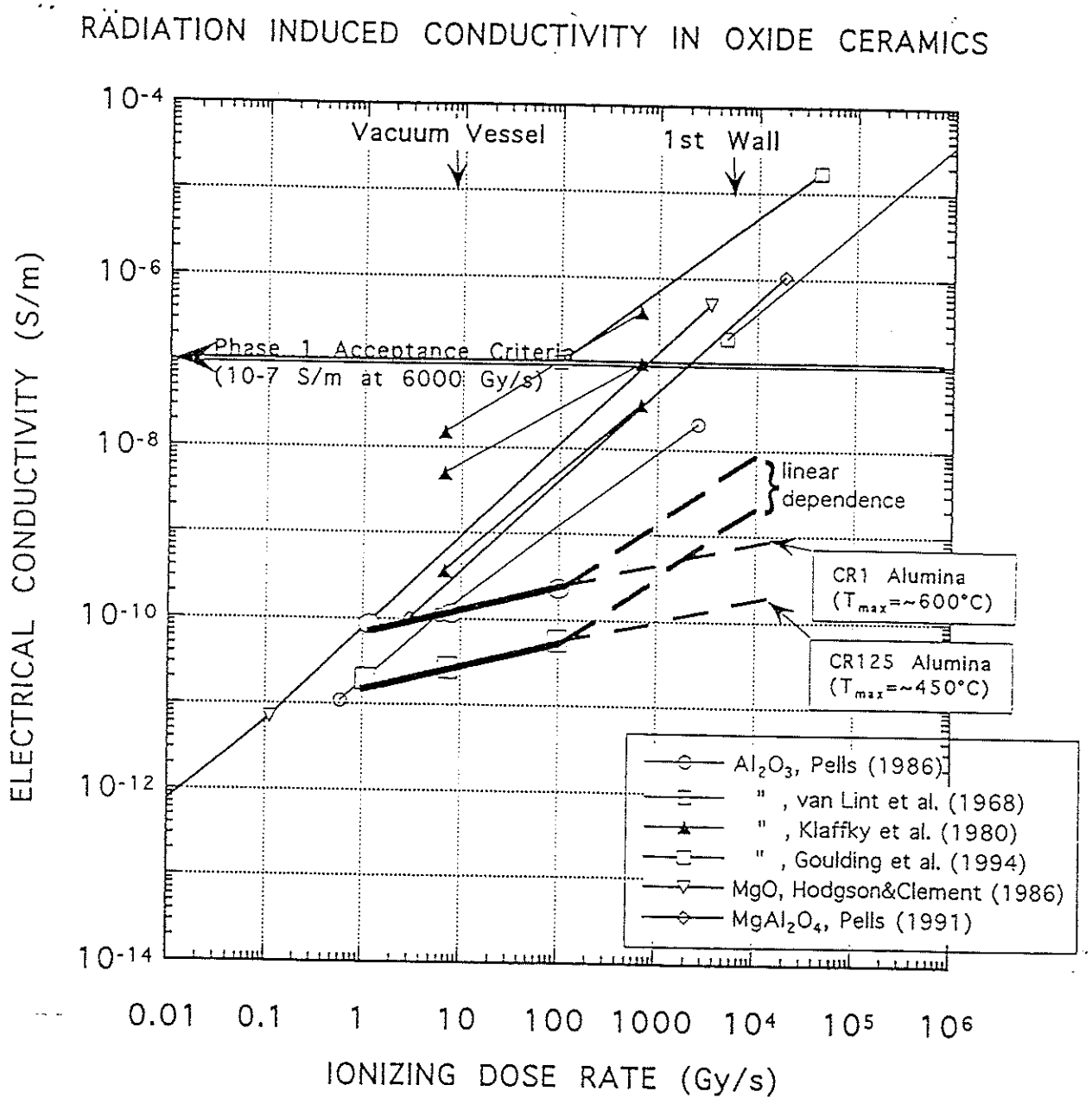

DISTRIBUTION LIST

1-5. R. W. McCullough, Delta M Corp., 1003 Clarence Larson Drive, Oak Ridge, TN 37830
6-7. Office of Scientific and Technical Information, P.O. Box 62, Oak Ridge, TN 37831
8. C. A. Valentine, Office of Technology Transfer, 701SCA, MS 8242
9-10. L. L. Snead, 4508, MS 6087
11. DOE-WFO, MS G209
12 P. L. Gorman, ORNL Site Office, 4500N, MS 6269
13. D. R. Hamrin, Lab Records, 4500N, MS 6285
14. A. J. Luffman, Office of Science and Technology Partnerships, 5002, MS 6416
15. R. A. Bradley, 4500S, MS 6161
16. A. C. Schaffhauser, 4500N, MS 6186
17. M. Upton, 4508, MS 6078